

This is an Open Access document downloaded from ORCA, Cardiff University's institutional repository:<https://orca.cardiff.ac.uk/id/eprint/179950/>

This is the author's version of a work that was submitted to / accepted for publication.

Citation for final published version:

Moon, Owen R., Newman, Andrew C., Alanazi, Abdullah S., Wehenkel, Sophie C., Gawel-Bęben, Katarzyna, Ivetic, Aleksandar, Price, David A. , Knauper, Vera and Ager, Ann 2025. TCR activation stimulates regulated intramembrane proteolysis of L-selectin by presenilin 1 and localized proteasomal degradation of the cytoplasmic tail. *Journal of Biological Chemistry* , 110473. 10.1016/j.jbc.2025.110473

Publishers page: <https://doi.org/10.1016/j.jbc.2025.110473>

Please note:

Changes made as a result of publishing processes such as copy-editing, formatting and page numbers may not be reflected in this version. For the definitive version of this publication, please refer to the published source. You are advised to consult the publisher's version if you wish to cite this paper.

This version is being made available in accordance with publisher policies. See <http://orca.cf.ac.uk/policies.html> for usage policies. Copyright and moral rights for publications made available in ORCA are retained by the copyright holders.



Journal Pre-proof

TCR activation stimulates regulated intramembrane proteolysis of L-selectin by presenilin 1 and localized proteasomal degradation of the cytoplasmic tail

Owen R. Moon, Andrew C. Newman, Abdullah S. Alanazi, Sophie C. Wehenkel, Katarzyna Gawel-Bęben, Aleksandar Ivetic, David A. Price, Vera Knäuper, Ann Ager

PII: S0021-9258(25)02323-3

DOI: <https://doi.org/10.1016/j.jbc.2025.110473>

Reference: JBC 110473

To appear in: *Journal of Biological Chemistry*

Received Date: 10 January 2025

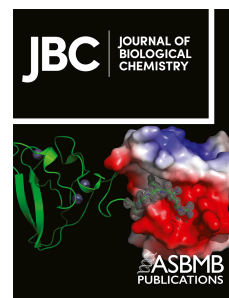
Revised Date: 8 June 2025

Accepted Date: 20 June 2025

Please cite this article as: Moon OR, Newman AC, Alanazi AS, Wehenkel SC, Gawel-Bęben K, Ivetic A, Price DA, Knäuper V, Ager A, TCR activation stimulates regulated intramembrane proteolysis of L-selectin by presenilin 1 and localized proteasomal degradation of the cytoplasmic tail, *Journal of Biological Chemistry* (2025), doi: <https://doi.org/10.1016/j.jbc.2025.110473>.

This is a PDF file of an article that has undergone enhancements after acceptance, such as the addition of a cover page and metadata, and formatting for readability, but it is not yet the definitive version of record. This version will undergo additional copyediting, typesetting and review before it is published in its final form, but we are providing this version to give early visibility of the article. Please note that, during the production process, errors may be discovered which could affect the content, and all legal disclaimers that apply to the journal pertain.

© 2025 THE AUTHORS. Published by Elsevier Inc on behalf of American Society for Biochemistry and Molecular Biology.



TCR activation stimulates regulated intramembrane proteolysis of L-selectin by presenilin 1 and localized proteasomal degradation of the cytoplasmic tail

Owen R Moon¹, Andrew C Newman¹, Abdullah S Alanazi^{1*}, Sophie C Wehenkel¹, Katarzyna Gawel-Bęben², Aleksandar Ivetic³, David, A Price^{1,4}, Vera Knäuper² and Ann Ager^{1,4}

¹Division of Infection and Immunity, School of Medicine, Cardiff University, Cardiff CF14 4XN, UK

²School of Dentistry, Cardiff University, CF14 4XY, UK

³Faculty of Life Sciences and Medicine, School of Cardiovascular Medicine and Metabolic Sciences, King's College London, London SE5 9NU, UK

⁴Systems Immunity Research Institute, Cardiff University, Cardiff CF14 4XN, UK

Owen Moon and Andrew Newman are first authors

*Current address: Department of Medical Laboratories, College of Applied Medical Sciences, Shaqra University, Shaqra, 11961, Saudi Arabia

Running title: Fate of L-selectin cytoplasmic tail following TCR activation

Correspondence: Ann Ager, Division of Infection and Immunity, School of Medicine, Cardiff University, Heath Park, Cardiff CF14 4XN, UK. Email: agera@cardiff.ac.uk.

Key words: ADAM17, CD62L/L-selectin, cell signalling, γ -secretase, imaging flow cytometry, regulated intramembrane proteolysis, T cell receptor (TCR)

Abbreviations:

ADAM: A metalloproteinase and disintegrin; APC: antigen presenting cell; CD62L: L-selectin; ECD: extracellular domain; FMO: fluorescence minus one; ICD: intracellular domain; LN: lymph node; MFI: median fluorescence intensity; MP: metalloproteinase; MRF: membrane-retained fragment; PS1: presenilin 1; RIP: regulated intramembrane proteolysis; TCR: T cell receptor

Abstract

Leucocyte (L)-selectin is essential for mounting protective immunity to pathogens. As well as regulating leucocyte recruitment, it also regulates their activation and differentiation inside tissues thereby shaping local immune responses. The biochemical signals that regulate these diverse functions of L-selectin are poorly understood. Leucocyte activation induces proteolytic shedding of L-selectin ectodomain (ECD) but the impact of ECD shedding on signalling downstream of L-selectin is not known. In T cells there is substantial overlap between signalling downstream of L-selectin and the TCR. Cross-linking of L-selectin stimulates phosphorylation of the cytoplasmic tail and forward signalling *via* the non-receptor tyrosine kinases Lck and Zap70. Cross-linking of TCR induces phosphorylation-dependent binding of PKC isozymes to L-selectin cytoplasmic tail and PKC α dependent shedding of ectodomain (ECD). To further understand the role of L-selectin in T cell biology, we used T cells to dissect the crosstalk between L-selectin and physiological TCR activation. We used a combination of imaging flow cytometry and biochemistry to localise L-selectin ECD and intracellular domain (ICD) following engagement of the TCR. We show that following ADAM17 dependent ECD shedding from the plasma membrane, the ICD containing transmembrane retained fragment undergoes intramembrane proteolysis by PS1 containing γ -secretase. Subsequent degradation of L-selectin ICD occurs via the proteasome in the vicinity of the plasma membrane. Regulated intramembrane proteolysis and rapid degradation of L-selectin ICD following TCR activation suggests that the turnover of L-selectin cytoplasmic tail is an important regulator of T cell co-stimulation by L-selectin.

Introduction

L-, E- and P-selectins comprise the selectin family of adhesion molecules on leucocytes and endothelial cells that are essential for leucocyte recruitment from the bloodstream to sites of inflammation and immunity(1). Leucocyte (L)-selectin or CD62L is a type 1 transmembrane C-type lectin expressed by the majority of circulating leucocytes. The best understood role for L-selectin on T cells is in recruitment or homing to lymph nodes (LN) which is required to mount protective immunity to pathogens. L-selectin binds to 6-sulpho sialyl Lewis X glycosylated ligands termed peripheral LN addressin (PNAd) on the luminal and basolateral surfaces of high endothelial venule (HEV) blood vessels. L-selectin-PNAd interactions enable shear stress-dependent tethering and rolling of T cells and subsequent transmigration across the vessel wall to enter the LN parenchyma (2).

Once inside LN, L-selectin has not been considered important for T cell function. However, *in vitro* studies have reported cross-talk between L-selectin and the TCR. L-selectin engagement stimulates T-cell proliferation (3), superoxide production (4), colony-stimulating factor 1 release (5), lytic activity (6) as well as β 1 and β 2 integrin-dependent adhesion (7-9). This may reflect the fact that L-selectin engagement stimulates several signalling pathways that are shared with TCR engagement such as activation of Lck, MAPK, c-abl, ZAP70, Ras and Rac (4,5). TCR engagement alone stimulates DAG/PKC dependent phosphorylation of serine residues in the cytoplasmic tail of L-selectin and stable binding of protein kinase C isozymes θ and α which are important regulators of TCR signalling (10). TCR engagement also stimulates ADAM17 dependent shedding of L-selectin ectodomain (ECD) from the T cell membrane (11). Why L-selectin ECD is shed is not completely understood but is a widely used marker to distinguish activated from naïve T cells due to loss of cell surface L-selectin. Important clues to the role of L-selectin shedding following TCR activation have come from studies comparing T cells expressing wild type and shedding-resistant forms of L-selectin. In mouse studies of virus immunity naïve CD8⁺ T cells unable to shed L-selectin show reduced TCR dependent clonal expansion inside draining LN after virus inoculation (11), delayed virus clearance by memory CD8⁺ T cells (12) and reduced clonal expansion in response to TCR engagement *in vitro*

(13). Human tumour-specific CD8⁺ cells expressing a non-cleavable form of L-selectin showed reduced lytic activity towards tumour cells which is associated with reduced degranulation and mobilisation of CD107a to the T cell membrane (14). Conversely, in a mouse model of adoptive T-cell cancer therapy, tumour-specific CD8⁺ T-cells unable to shed L-selectin were better able to restrict the growth of solid and disseminated tumours than wild type T-cells (13). The beneficial effects of T-cells unable to shed L-selectin was unrelated to improved recruitment from the bloodstream into tumours or involved lymph nodes but, instead, correlated with early peptide-MHC dependent activation of T-cells in the tumour microenvironment and in involved lymphoid organs (13). Together, these studies suggest that signals transmitted by L-selectin during TCR-engagement regulate biological responses in T-cells independently of its homing function. Moreover, L-selectin dependent signalling is regulated by shedding of the ECD.

What then could be the impact of ADAM17 dependent proteolytic shedding of L-selectin on T cell activation? Several possibilities can be envisaged which are not mutually exclusive: Firstly, the released ECD competes with ligands on antigen presenting cells and antagonises L-selectin dependent signals in adjacent T-cells. Secondly, loss of L-selectin ectodomain immediately shuts off all signalling in T-cells that is initiated and sustained by ligand binding or thirdly, the membrane-retained fragment (MRF) of L-selectin undergoes regulated intramembrane proteolysis and the released C-terminal intracellular domain (ICD) propagates TCR-dependent initiated signals.

In this study we determined the fate of the cytoplasmic tail in TCR-activated T cells using a combination of imaging flow cytometry and biochemical analysis. We report that following TCR clustering and protein kinase C dependent activation of ADAM17, cleavage of the L-selectin ectodomain enables intramembrane cleavage of the MRF by presenilin 1 containing γ -secretase and proteasomal degradation of the ICD in a peri-plasma membrane location. Our findings that L-selectin cytoplasmic tail is poised for rapid turnover in the membrane of activated T-cells and suggests that it actively shapes TCR-driven biological responses.

Results

1. Generation of L-selectin-V5-His to track the cytoplasmic tail in TCR-activated T-cells

Our previous work showed that activation of the TCR on CD4+ T cells using MHC Class II binding bacterial superantigen staphylococcus enterotoxin B (SEB) and on CD8+ T cells by peptide-MHC1 stimulates ADAM17 dependent ectodomain proteolysis of L-selectin in human and mouse cells (11). To monitor the accumulation of cleaved fragments of L-selectin after ADAM17 shedding of ECD, we expressed L-selectin tagged with a V5-His tag at the intracellular carboxy terminus (Fig. 1A) in MOLT-3 T cells that do not express endogenous L-selectin. This provides a clean background in which to study L-selectin-V5-His using V5-antibodies for western blotting of cell lysates to detect C-terminal fragments. To study the impact of physiological TCR engagement on L-selectin biology, MOLT-3 T cells expressed 868 TCR which recognises HIV antigenic SLYNTIATK (SLY) peptide bound to HLA-A*02 on antigen presenting cells (APC). Transduced MOLT-3 T cell lines co-expressing L-selectins and 868 TCR were subjected to rigorous cell biological and biochemical characterization to ensure that C-terminal tagging of L-selectin with the V5-His tag did not interfere with ADAM17 dependent L-selectin ECD shedding. We have reported dose-dependent shedding of non-tail tagged L-selectin following ligation of 868 TCR by SLY peptide pulsed APC which is completely inhibited by DA1(12) antibody to human ADAM17 (11). Engagement of the 868 TCR with SLY peptide-MHC on APC stimulated dose-dependent shedding of L-selectin-V5-His from the cell surface measured by live cell imaging (Fig 1B, Fig S1). The dose-response curve was similar to that of non-tagged L-selectin with 10^{-6} M SLY peptide causing maximal loss of L-selectin from the cell surface, which was blocked by the synthetic metalloproteinase inhibitor Ro 31-9790 (Fig. 1B).

To detect ADAM17-generated fragments of L-selectin in cell lysates of TCR-activated cells we probed Western blots with V5 antibody. We used T cell activator beads coated with anti-CD3/28 instead of peptide-pulsed antigen presenting cells to avoid diluting T cell lysates with APC lysates for detection purposes. In the absence of TCR stimulation, a broad band of ~ 60 kDa was routinely detected in cell lysates (Fig. 1C, control beads). Following TCR-activation the ~60kDa band was reduced and a single cleavage product of ~8 kDa was detected. Inclusion of an inhibitory ADAM17

antibody (D1(A12) (15), retained the ~60kDa band and prevented the appearance of the smaller band showing clearly that the latter represents the ADAM17 cleavage product. Together these results show that the ~60kDa band represents full length L-selectin-V5-His expressed in MOLT-3 T-cells and that it is cleaved by ADAM17 to generate a single V5-tagged, cytoplasmic tail containing species of ~8 kDa. Although western blotting of whole cell lysates does not distinguish between membrane and cytoplasmic proteins, we reasoned that by analogy with other type 1 membrane proteins cleaved by membrane inserted ADAMs, the ICD containing product is a membrane retained fragment (MRF). In some experiments, a faint 8 kDa band was detected in non-activated T-cells expressing L-selectin-V5-His (Fig. 1C, control beads). This likely reflects the low levels of homeostatic or basal L-selectin shedding known to occur in T-cells, which we have shown to be independent of ADAM17 activity (11).

The kinetics and dose response of pharmacological activation of ADAM17 by PMA and shedding of L-selectin from MOLT-3 T-cells expressing L-selectin-V5-His were compared directly with cells expressing non-tagged L-selectin (Fig. 1D). Using maximal levels of 300nM PMA (Fig. S1) the kinetics and dose-response of L-selectin downregulation from the surface of MOLT-3 T cells were not affected by the V5-His cytoplasmic tagged tail (Fig 1D, Fig S1). The magnitude of PMA induced downregulation of cell surface L-selectin was similar to that induced by TCR engagement (Fig 1D, middle and right-hand panels). These results show that the V5-His tag does not attenuate ADAM17 dependent shedding of L-selectin following TCR activation by peptide-MHC complexes and anti-CD3/CD28 or PMA.

2. TCR stimulation induces both ADAM17 and γ -secretase dependent proteolysis of L-selectin

Most Type I membrane proteins that undergo ECD shedding by ADAMs are susceptible to subsequent proteolytic cleavage within their transmembrane domains by the γ -secretase complex (16) (17). To determine if the membrane retained fragment of L-selectin generated by ADAM17 shedding of the ECD is susceptible to γ -secretase we tested ADAM17 activation in the presence and absence of γ -secretase inhibitors L-685 (18) or DAPT (19). We hypothesised that TCR engagement

would stimulate rapid (within minutes) sequential proteolysis of L-selectin by ADAM17 and γ -secretase. To understand the role of L-selectin in T-cell function/biology we wanted to follow the fate of the ICD of L-selectin to determine whether it relocates to another cellular compartment or is degraded. To do this we used a range of ADAM17 activating stimuli to overcome limitations of conjugate formation between T cells and peptide-pulsed APC, which could dilute out or obscure signals during biochemical analysis. We first tested TCR activation using MOLT-3 T-cells transduced with L-selectin-V5-His using T-cell activator beads coated with CD3/CD28 in the presence or absence of γ -secretase inhibitor L-685. Kinetic analysis showed that TCR activation induced detectable loss of L-selectin from the cell surface within the first 5 min and maximal loss at 15 min (Fig. 2A B). Inclusion of L-685 had no effect on TCR-dependent ECD shedding of L-selectin from the T cell surface (Figs. 2A, B) and release of soluble L-selectin (Fig. 2C). Analysis of cell-free supernatants confirmed that TCR engagement stimulated rapid release of L-selectin over the first 15 mins (Fig 2C). These results show that TCR stimulation activates ADAM17 at early time points, causing rapid cleavage of L-selectin, independent of γ -secretase activity. Although control beads had no effect on cell surface L-selectin, constitutive shedding was evident by release of small quantities of soluble L-selectin (Fig. 2C, control beads), which we and others have shown to be independent of ADAM17 (11,20,21). ADAM17-dependent shedding of L-selectin induced by PMA was also unaffected by inhibition of γ -secretase activity but blocked by the inhibitory ADAM17 antibody (Figs. 2D, E).

Analysis of L-selectin-V5-His by Western blotting showed that in control bead treated T-cells the 60 kDa doublet representing full length L-selectin-V5-His was stable over a 60 min time course (Figs. 3A, D). In TCR-activated T-cells, the 60 kDa band intensity decreased between 5 and 15 min, when it was no longer detectable (Fig. 3B, E). The ADAM17 MRF cleavage product was not detectable prior to T cell activation or in control T-cells, however it was detected at 5 min after TCR activation (Figs. 3 B, G). The MRF fragment decreased over time and was barely detectable at 60 min (Fig. 3B, G). In line with observations by flow cytometry, inhibition of γ -secretase did not prevent TCR-induced loss of full-length L-selectin-V5-His over the 60 min time course (Fig 3C, F). However, L-685 stabilized the MRF (Figs. 3C, H). These results show that TCR stimulation initiates

intramembrane proteolysis of the MRF fragment by γ -secretase. In the absence of L-685, we were not able to detect smaller γ -secretase generated fragment of L-selectin-V5-His by in cell lysates. To confirm that the generation of the MRF fragment was independent of the cell stimulation method, we used PMA treatment in the presence or absence of the γ -secretase inhibitor L-685 or ADAM17 inhibitory antibody to determine MRF fragment levels by Western blotting, which confirmed findings from TCR activated cells that L-685 stabilized the MRF and that generation of the MRF is ADAM17 dependent (Fig. 3I, J). Endogenous and non-tagged L-selectins behaved similarly in response to PMA in that the MRF was stabilized by γ -secretase inhibition (Fig. S2).

3. PS1 but not PS2 caused cleavage of the ADAM17 membrane retained L-selectin product

To confirm intramembrane proteolysis of L-selectin we used a genetic approach of cells deficient in presenilin (PS), the catalytic subunit of γ -secretase. There are 2 isoforms of presenilin, PS1 and PS2 both of which have been shown to cleave type I transmembrane proteins following cleavage by ADAM17 (17). To study their role in intramembrane proteolysis of L-selectin, we used PS1/2 double null mouse embryonic fibroblasts cells (MEFs) as well as wild type MEFs which express both PS1 and PS2, confirmed by immunoblotting with C-terminal PS1 or PS2 antibodies, (Fig. 4A, B) (22,23). Wild type and PS1/2 null MEFs were transiently transfected with L-selectin-V5-His expression construct and subsequently treated with either γ -secretase inhibitor L-685, metalloproteinase inhibitor Ro 31-9790 or DMSO solvent.

Wild type and PS null MEFs express relatively high levels of mouse ADAM17, thus activation of ADAM17 activity was not necessary in these cells as cleavage of L-selectin-V5-His was obvious in basal conditions due to limited detection of full-length L-selectin-V5-His (Fig. 4C). In wild type MEFs L-685 treatment enriched the MRF fragment, while Ro 31-9790 pretreatment prevented its formation. In contrast, L-685 treatment of PS1/PS2 double null cells did not have any effect on the band intensities for the MRF fragment, which was at the same level as the solvent control or Ro 31-9790 treated sample (Fig. 4C, D). Next, we used PS1/PS2 double null cells transfected with either PS1 or PS2 (Fig. 4A, B) to establish which PS isoform was responsible for MRF fragment cleavage. Following transient transfection with the L-selectin-V5-His expression construct full length L-selectin was at or below the level of detection in cell lysates of untreated PS1 or PS2 singly expressing MEF

cells (Fig. 4E). Incubation with the broad spectrum MMP/ADAM inhibitor Ro 31-9790 for 60 mins prior to cell lysis had no effect on full length L-selectin levels. However, the MRF was detected in cell lysates of both PS1 and PS2 expressing MEFs, which was decreased by incubation with Ro 31-9790 confirming its identity as a metalloproteinase (MP) cleavage product.

In PS1 expressing MEFs, there was a significant enrichment of the MRF-fragment upon L-685 treatment when compared to DMSO control (Fig. 4E, F). In contrast, there was no change in MRF product levels between DMSO and L-685 treated cells in PS2 expressing MEFs (Figs. 4E, F). These results indicate that PS1 is responsible for intramembrane proteolysis of the MRF fragment of L-selectin. Full length L-selectin was not detected following inclusion of the γ -secretase inhibitor L-685 (Fig. 4 C, E) consistent with its lack of effect on L-selectin-V5-His shedding from the T-cell surface (Fig. 2B).

These results suggest that the MRF fragment of L-selectin generated by ADAM17 is subsequently proteolyzed by the intramembrane multi-subunit protease complex, γ -secretase containing PS1 but not PS2.

4. Fate of L-selectin cytoplasmic tail following ADAM17 and PS1 dependent proteolysis

To determine the subcellular localisation of ADAM17 and γ -secretase generated fragments of L-selectin we used imaging flow cytometry and analysed subcellular compartments in MOLT-3 T cells for L-selectin-V5 signals. This technique has the advantage of testing multiple fluorophores on the same cell simultaneously and avoids the requirement to immobilise non-adherent T-cells for conventional confocal microscopy. Furthermore, imaging flow cytometry allows high throughput analysis as every cell is imaged and analysed. To perform this analysis, we selected PMA as a pharmacologic mimic of TCR/PKC dependent L-selectin shedding. This approach avoids complications where activator beads or T-cell-APC conjugates, would make image analysis more complex. By staining for sub-cellular compartments (membrane, nucleus, and the lysosome) and the tail of L-selectin, we sought to determine how these fluorescence signals co-localise. The imaging flow cytometry IDEAS software package uses a log-transformed Pearson's correlation co-efficient to evaluate the similarity in the distribution of fluorescence between two probes which is reported as a

'similarity score' (24). The similarity score feature is designed for use within user-defined sub-cellular compartments or 'masks'.

To determine whether the V5 tag on L-selectin was within the membrane in activated MOLT-3 T cells we searched for an endogenous cell surface marker in MOLT-3 T cells. We stained live MOLT-3 T cells for extracellular CD69 to locate the plasma membrane's outer leaflet and then fixed and permeabilized the cells and stained for the intracellular V5 tag on L-selectin to define the inner membrane leaflet (Fig 5A, CD69). We plotted the fluorescent signal intensity against the mask number for CD69 and V5 signals and created membrane and intracellular masks (Fig. S3). Within the intracellular mask distinct intracellular compartments, such as the lysosome (CD107a, lysosome marker) or the nucleus (NucBlue signal) were used to assess whether the cytoplasmic tail of L-selectin co-localized to any of these intracellular compartments (Fig. 5A). We found CD69 is constitutively expressed in L-selectin+ MOLT-3 T cells and CD69 expression levels are unchanged following PMA treatment for up to 15 min (Fig S3). Therefore, we used CD69 as a membrane marker for these studies. The subcellular location of L-selectin ICD in the absence and presence of γ -secretase inhibitor L-685 was determined 0, 5, 10 and 15-minutes post-PMA stimulation by determining similarity scores between L-selectin ICD and sub-cellular compartments (membrane, nucleus, and the lysosome).

Cells positive for CD69, CD107a and the L-selectin tail (by V5-His tag staining) relative to the isotype control (Fig. S4) were 'AND-gated' and triple positive events were assessed for their median similarity scores between pairs of markers within the relevant cellular compartments. Representative staining (Fig. 5A) and normalized frequencies plotted against similarity scores for the 15-minute time point with PMA (activated) or DMSO control (unactivated) T cells are shown (Fig. 5B-D, control: black unfilled histograms; PMA: green filled histograms). Similarity scores for L-selectin-ICD V5-signal and the CD69 membrane signal in the absence of activation were well above 1 (Fig. 5B, black histogram) and averaged 1.84 (Fig 5H, black symbols). This supports the findings of conventional flow cytometry where full length L-selectin, i.e., before the ECD is shed, is detectable at the surface of MOLT-3 T-cells under basal conditions (Figs.1 and 2). In comparison, similarity scores for L-selectin-ICD V5-signal and the lysosome ranged from 0.8 to 1.0 in unactivated cells (Fig. 5C, black

histogram, Fig 5I, black symbols). Furthermore, similarity scores for L-selectin-ICD V5-signal and the nucleus in unactivated cells were consistently less than 0 (Fig. 5D, black histogram; Fig. 5J black symbols). Together these findings show that L-selectin prior to cell activation is preferentially located in the plasma membrane of MOLT-3 T-cells.

The similarity score between the L-selectin tail and CD69 in the membrane mask decreased at 15 minutes after PMA addition (Fig. 5B, green filled histogram, black arrow). The similarity score was reduced to 1.66, although it remained above 1 (Fig. 5H, green symbols). PMA had no effect on similarity scores between L-selectin-ICD V5-signal and the lysosomal compartment (Fig. 5C, 5I;<1) nor in similarity scores between L-selectin-ICD V5-signal and the nuclear compartment (Fig. 5D, 5J;<0), suggesting that the cleaved L-selectin-ICD V5 MRF fragment does not co-localize with either the lysosomal or nuclear compartments. Inclusion of the γ -secretase inhibitor L-685 stabilized similarity scores between L-selectin-ICD V5-signal and the plasma membrane in the presence of PMA at 1.84 which was similar to solvent control levels (Fig. 5E, green filled histogram, white arrow; Fig. 5H, green symbols) suggesting that γ -secretase activity is essential for loss of ICD from the plasma membrane. L-685 had no effect on co-localisation of L-selectin-ICD V5-signal with either lysosomal or nuclear markers in the presence of PMA (Fig. 5I, 5J).

Interestingly, staining for V5 tag revealed distinct intracellular 'deposits' or spots of L-selectin-V5 signal (Fig 5A). Some evidence for co-localization between L-selectin-ICD V5-signal and CD107a was seen in a small subpopulation of cells which had similarity scores >1 (Fig. 5C). Although we found no increase in similarity scores between L-selectin-ICD V5-signal and CD107a following PMA treatment, it is possible that L-selectin-ICD moves to an intracellular compartment which is not detected by CD107a staining. We therefore determined if the loss of ICD co-localization with the membrane in response to PMA was accompanied by an increase in the number of spots per cell as the L-selectin-V5 cytosolic tail is cleaved and potentially moves away from the membrane and into a distinct intracellular compartment. However, no increase in the number of intracellular spots was seen at 15 minutes post PMA addition in the presence or absence of L-685 (Fig. S4). Intracellular spots may represent the high levels of Golgi-associated full-length L-selectin produced in lentivirally transduced T cells.

5. Degradation of L-selectin ICD following ADAM17 and PS1 proteolysis

We hypothesised that the loss of L-selectin tail staining from the membrane and lack of accumulation in an intracellular compartment was due to degradation of the tail. To address this hypothesis, a lentiviral vector encoding human L-selectin tagged with GFP instead of V5 (Fig. 1A, (25)) was used to transfect the parental L-selectin negative MOLT-3 T cell line and these cells were treated with PMA for 15 minutes prior to imaging flow cytometry.

PMA treatment was sufficient to reduce whole-cell L-selectin-GFP fluorescence in live cells (Fig. 6A) whilst CD69 levels remained stable (Fig. 6B). For PMA-treated cells, the GFP median intensity decreased significantly regardless of whether the cells were live or fixed and then permeabilised (Fig. 6A, C, compare filled green histograms to black lined histograms). The live cells appeared dimmer by median fluorescence intensity measurements relative to cells fixed and then permeabilised, but this was due to the presence of GFP^{dim} cells, and not to the loss of GFP^{bright} cells (Fig. 6A, C). PMA induced a ~30% loss in L-selectin-GFP signal in live cells showing clearly that L-selectin ICD signal is reduced following PMA activation as found for V5-tagged ICD (Fig 6E). The loss of L-selectin-GFP signal in fixed/permeabilised cells was similar (Fig 6E). As shown in the representative histograms, CD69 remained stable following PMA treatment in both live and fixed/permeabilised cells and therefore could be used as a membrane marker in experiments with this MOLT-3 cell line expressing GFP-tagged L-selectin (Fig. 6B, D). V5-His tagged L-selectin behaved similarly in that whole cell fluorescence intensity decreased in response to PMA treatment (Fig. 6F) and the fold changes in GFP and V5 fluorescence in fixed and permeabilised cells were not different (Fig 6G).

Together, these findings support the conclusion that loss of L-selectin ICD tail from the membrane is not due to leakage from the cells during fixation and permeabilisation. The fact that both V5- and GFP- signals decrease suggest that loss of V5 signal is not simply due to a binding partner preventing access of antibody to the tail. Rather, the PMA-induced loss in fluorescence is likely due to degradation of the MRF-fragment.

6. Proteasomal degradation of L-selectin ICD following TCR activation

Our findings thus far support the hypothesis that TCR induced activation of ADAM17 caused cleavage of the ectodomain of L-selectin, the membrane retained fragment undergoes proteolysis by γ -secretase and the ICD is subsequently degraded. Imaging flow cytometry showed that the L-selectin ICD is rapidly lost from the plasma membrane as early as 15 min after TCR stimulation and provided evidence of L-selectin ICD degradation. To confirm experimentally that the L-selectin ICD is degraded we used western blotting and determined the impact of the proteasomal, endo-lysosome and autophagosome on L-selectin ICD in TCR stimulated cells. We used MOLT-3 T cells expressing the 868 TCR and V5-His tagged L-selectin and stimulated the cells with SLY cognate peptide pulsed antigen presenting cells to activate the TCR leading to sequential proteolysis of L-selectin by ADAM17 and γ secretase. 868 TCR+, L-selectin-V5+ MOLT-3 T cells incubated with the antigen presenting cells pulsed with NLV peptide were used as negative controls. Although C1R antigen presenting cells express endogenous L-selectin, it is not tagged with V5 and therefore not detected by western blot analysis with the V5 antibody.

Samples were analysed 10 min after activation since the MRF is rapidly lost from whole cell lysates by 15 min (Fig. 2). At this early time point, changes in full length L-selectin were not detectable (Fig. 7A, B). As found using polyclonal T cell activation using CD3/28 activator beads (Fig 2), ADAM17 activation by peptide-MHC engagement of TCR did not generate a detectable MRF unless γ -secretase activity was inhibited (Fig. 7A, C) whereas the control peptide NLV did not stimulate ADAM17 dependent shedding of L-selectin and therefore MRF was not detected even in the presence of L-685 (Fig. 7A, C). We tested the proteasome inhibitor MG132 to determine if this would stabilise a smaller L-selectin fragment representing the ICD released by γ secretase. T cells were pretreated with MG132 and then stimulated with peptide-MHC carrying either activating SLY or NLV control peptide in the presence or absence of MG132. MG132 enriched an L-selectin-ICD fragment of around 8 kD in SLY but not in NLV control peptide treated T cells (Fig. 7A, C). Interestingly the L-selectin ICD fragment stabilised by proteasomal inhibition was the same size as the MRF stabilised by L-685 and a smaller fragment predicted to represent the γ -secretase generated ICD was not detected. The effects of either MG132 or L-685 alone to prevent loss of the MRF were equivalent (Fig. 7C). To determine if L-685 and MG132 had additive effects on the MRF, T cells were pretreated

with both inhibitors and TCR stimulated with peptide-MHC as above. The combination of L-685 and MG132 enriched an L-selectin-ICD fragment of around 8kD in SLY but not in NLV treated T cells (Fig. 7A). However, this was not significantly different from T cells treated with vehicle control DMSO alone (Fig. 7A, C). There was no evidence for endo-lysosomal degradation or autophagic recycling of L-selectin MRF since inclusion of lysosomal and autophagy inhibitors did not stabilise the L-selectin MRF in PMA stimulated cells (Fig. 7D, E). Together these findings demonstrate that the γ -secretase generated ICD of L-selectin undergoes rapid proteasomal degradation in close proximity to the plasma membrane.

Discussion

In this study we have used a combination of subcellular imaging, genetic and pharmacological inhibition as well as biochemical analysis to follow the fate of the cytoplasmic tail of cell surface L-selectin in T cells following engagement of the TCR. Our studies show that cell surface L-selectin is proteolyzed exclusively by ADAM17, the L-selectin fragment remaining in the membrane is subsequently cleaved by presenilin 1 (PS1) and the intracellular domain (ICD) undergoes proteasomal degradation in or adjacent to the plasma membrane (Fig. 8). We have already demonstrated that ADAM17 dependent shedding of L-selectin regulates clonal expansion of T cells since T cells unable to shed L-selectin following engagement of the TCR show markedly reduced T cell proliferation *in vitro* and *in vivo*. The demonstration here that proteasomal degradation of L-selectin ICD is a consequence of shedding raises the possibility that proteasomal turnover of L-selectin ICD actively regulates T cell function.

The cytoplasmic tail of L-selectin plays an active role in controlling shedding of the ectodomain. Constitutive binding of Calmodulin (CaM) to hydrophobic residues Ile³⁵² and Ile³⁵⁴ in L-selectin ICD causes resistance to L-selectin shedding (26), (27). Phosphorylation at Ser³⁶⁴ causes dissociation of CaM and facilitates ectodomain proteolysis (25). Additionally, differential binding of ezrin and moesin to Arg³⁵⁷ and Lys³⁶² in the ICD regulate shedding of L-selectin (28), (29). In our studies, L-selectin was fused to a carboxy terminal V5-His tag, which potentially could have hindered interaction with these protein binding partners abrogating proteolysis. Therefore, we confirmed that the V5-His tagged L-selectin was susceptible to proteolysis after TCR-activation. Our data showed loss of cell surface expression for both V5-His and non-tagged L-selectin after TCR-activation, which was blocked by Ro 31-9790 and the inhibitory anti-ADAM17 antibody D1(A12). TCR-activated cells also showed loss of full-length L-selectin and generation of the MRF by immunoblot analysis which was blocked by the anti-ADAM17 antibody (D1(A12)). Pharmacological activation of ADAM17 by PMA showed similar dose-responses and time courses for ectodomain shedding of non-tagged and tagged L-selectin. The V5-His tag did not interfere with γ -secretase dependent degradation since endogenous, non-tagged and tagged L-selectin MRF were all enriched by treatment with γ -secretase inhibitors. Collectively, our data confirmed that the C-terminal V5-His tag of L-selectin did not

interfere with ADAM17 or γ -secretase dependent proteolysis after TCR activation. This agrees with previous studies where L-selectin-GFP undergoes PMA induced ectodomain shedding (25).

Flow cytometry and immunoblot analysis showed that activation of the TCR caused ectodomain proteolysis of L-selectin independently of γ -secretase activity since the MRF and released ECD were detectable within the first 10-15 mins in the absence or presence of γ -secretase inhibitors. These results confirmed that after TCR stimulation, ADAM17 sheds L-selectin at the ectodomain before further proteolytic processing. Immunoblot analysis showed that the ADAM17 product of L-selectin detected at 5 min post-TCR stimulation decreased from 5 min to 60 min, which was blocked by the γ -secretase inhibitor L-685. Together, these results showed that TCR stimulation induces sequential proteolysis of full-length L-selectin first by ADAM17 and then by γ -secretase.

Presenilin (PS) is the catalytic subunit of the γ -secretase multiunit complex (30). γ -secretase assembly into a functional complex occurs in a stepwise manner in the endoplasmic reticulum, where presenilin PS undergoes endoproteolysis between residues Thr²⁹¹ and Ala²⁹⁹ to generate a 30 kDa N-terminal fragment and a 17 kDa C-terminal fragment which form the catalytically active enzyme (31), (32). There are two isoforms of PS, PS1 and PS2, which show some substrate selectivity. For instance, APP and Notch are proteolyzed by both PS1 and PS2 (33), (34), (22), whereas ErbB4 is selectively proteolyzed by PS1 (35). To determine whether the MRF product of L-selectin was cleaved by PS1 and/or PS2, PS deficient MEF cells were complemented with PS1 and/or PS2. We found that PS1, but not PS2 expression was required for proteolysis of the L-selectin MRF product. Further studies will be required to determine if PS1 is constitutively active in T-cells or requires TCR engagement for endoproteolytic activation.

To dissect the role of L-selectin shedding in TCR induced signalling we followed the fate of L-selectin ICD generated by γ -secretase. L-selectin ICD was not detectable as a distinct molecular species separable from the larger ICD containing membrane retained fragment by western blotting. ICDs of other type I transmembrane proteins released by γ -secretase are often not readily detectable by western blot analysis. Pretreatment of cells with proteasomal inhibitors for 5 to 24 h prior to cell lysis enabled detection of ICDs released from full-length proteins, such as Notch in epithelial cells (36),

LDLR in HEK and neuroglioblastoma cells (37) (38), MHC Class I in CHO cells (39) and protocadherin in HEK cells (40). Contrastingly, degradation of the ICD of APP is not blocked by proteasome or lysosomal inhibitors (41). Instead, the APP ICD is rapidly cleared by the insulin degrading enzyme, a cytoplasmic metalloproteinase that proteolyzes small polypeptides (42). Studies have overcome degradation of endogenous ICDs by overexpressing cDNAs encoding the ICDs of APP (AICD) and Notch (NICD) or constitutively active Notch and demonstrated translocation of ICDs to the nucleus where these fragments act as transcriptional factors. Overexpressed APP ICD in the cytoplasm forms a multimeric complex with Fe65 nuclear adaptor protein and the histone acetyltransferase Tip-60 inducing transcription of APP and other genes (43) (44). Comparably, ICD of constitutively active Notch binds to the transcription factor CSL in the nucleus and binds to DNA (45). In other studies, phosphorylated Notch ICD is ubiquitinated and degraded by the proteasome in the nucleus (46), (47). Based on these findings, we hypothesised that the L-selectin ICD is either rapidly degraded and/or trafficked to a subcellular compartment which was not solubilized during cell lysis and therefore L-selectin could not be detected by western blotting.

Imaging flow cytometry was used to track the subcellular location of cytoplasmic tail of L-selectin in T cells following activation of ADAM17. To achieve this, a method for distinguishing plasma membrane from intracellular cytoplasm in T cells was required. Antibodies that bind to the ECD of L-selectin and CD69 in the outer lipid bilayer and antibodies to V5, which binds to the tail of CD62L-V5 in the inner lipid bilayer were used to distinguish plasma membrane from cytoplasm in 868 TCR+ MOLT-3 cells. Interestingly, CD69 which was constitutively expressed by 868 TCR+ MOLT-3 cells was not affected by PMA, whereas L-selectin ECD was shed and therefore CD69 was used as a membrane marker. A range of parameters were measured including whole cell median fluorescence intensity values, as in conventional flow cytometry, as well as the median fluorescence intensity in the membrane. In addition, the lysosomal compartment was defined using CD107a and the nucleus with NucBlue, which allowed us to quantify colocalization of L-selectin with the membrane and distinct intracellular compartments as a similarity score between specific fluorophore pairs.

Imaging flow cytometry showed clearly that the ECD of L-selectin was shed from the plasma membrane/cell surface within 15 min following activation of ADAM17, as demonstrated by

conventional flow cytometry. The similarity of fluorescence associated with the L-selectin tail and the membrane marker CD69 significantly decreased at 15 minutes, indicating that the V5-tagged tail is lost from the plasma membrane, which was prevented by inclusion of the γ -secretase inhibitor L-685. This indicates that the γ -secretase complex is co-located where its substrate, the ADAM17 dependent MRF is generated. V5 detection in lysosomal and nuclear compartments did not change following γ -secretase activation suggesting that the V5-tagged tail did not relocate to these compartments. To determine if loss of V5-tail signal was due to degradation, we used L-selectin-GFP, which enabled analysis of live cells and avoided fixation and permeabilization processes required to detect the V5 tag. In live cells, GFP signal was reduced by ADAM17 activation showing that loss of L-selectin tail is due to degradation. In fixed and permeabilised cells ADAM17 activation also induced a loss of L-selectin-GFP confirming that L-selectin-GFP behaves similarly to L-selectin-V5. The reduction in GFP- and V5-tail signals were similar. Together these results demonstrate that loss of V5 signal from the membrane is not an artefact due to procedures used for detection but due to degradation.

To determine whether the L-selectin tail is degraded by the proteasome, we analysed the effect of MG132 on L-selectin-V5 fragments in TCR-activated MOLT-3 cells by western blotting. Inclusion of MG132 enriched a single band of 8 kDa in SLY peptide activated T cells, which was a similar in size to the MRF seen in γ -secretase inhibited cells. This raised the possibility that the MRF undergoes direct proteasomal degradation that may not require prior release of ICD by γ -secretase. To determine if MRF undergoes proteasomal degradation when γ -secretase is blocked, we used a combination of MG132 and L-685. Interestingly, the combination of MG132 and L-685 did not further enrich 8 kDa fragment levels over that with either MG132 or L-685 alone. Instead, MG132 and L-685 in combination had a reduced effect and although enrichment of the 8 kDa fragment was seen but was not significantly different from control cells. This could be because the inhibitors interfere with each other's activity which will require further investigation. There was no evidence for removal of the ICD-containing MRF via lysosomal or autophagic pathways. There was also no evidence of relocation of L-selectin ICD to the nucleus. However, Notch ICD is below the level of detection in the nucleus of intact cells and requires overexpression to detect its transcriptional activity (45). The

L-selectin ICD contains a conserved C terminal PY motif. Studies have shown that C terminal PY motifs act as nuclear import signals for Hrp-1 and Nab-2 (48) so could potentially also regulate nuclear import of L-selectin ICD. Further studies will therefore be required to determine if L-selectin ICD has transcriptional activity.

It is curious that no new proteolysis product corresponding to the γ -secretase cleaved ICD could be observed either by western blotting or by imaging flow cytometry. This raises the possibility that the cleaved ICD stays associated with MRF in the membrane and is degraded in a membrane-associated proteasome. It is also possible that a cleaved ICD in TCR activated cells is phosphorylated on Ser³⁶⁴ and Ser³⁶⁷ (25) and the increase in negative charge results in co-migration of phosphorylated ICD with the MRF on SDS-PAGE analysis.

Proteasomal degradation of L-selectin ICD would require prior ubiquitination by a E3 ubiquitin ligase. Interestingly, basal turnover of full-length L-selectin in T cells is not regulated by proteasomal degradation (49). However, K5, a E3 ubiquitin ligase in Kaposi sarcoma herpes virus has been shown to downregulate full length L-selectin in lymphocytes. L-selectin downregulation is dependent on ubiquitination of lysines in the ICD of L-selectin but is not dependent of ECD shedding. Moreover, KSHV E3 ubiquitin ligases target full length membrane proteins for internalisation and endo-lysosomal degradation (50),(51). Degradation of L-selectin MRF was not stabilised by lysosomal inhibition and therefore endo-lysosomal degradation of internalised MRF is unlikely. Further studies will be required to determine whether the L-selectin ICD generated following TCR activation is a cognate substrate for the ubiquitin-proteasomal system (UPS) and, if so, which of the > 600 E3 ubiquitin ligases in the human genome is involved (52).

The biochemical relevance of PS1 proteolysis of the ADAM17 generated L-selectin membrane-retained fragment and subsequent proteasomal degradation of the cytoplasmic tail in activated T cells are currently unknown. ADAM17-dependent shedding of L-selectin plays a significant role in controlling T cell dependent immunity to tumours (13) as well as to viruses (53), (12). It is known that L-selectin shedding controls vascular recruitment and homing of activated T cells to sites of immune activity (54). In addition, L-selectin shedding also controls T cell proliferation (11) and lytic activity (14) which are both processes that are not related to homing.

Interestingly, imaging studies have shown that TCR is located on microvilli where L-selectin is selectively localised (55). This raises the possibility that TCR and L-selectin co-location facilitates crosstalk between these two receptors. It has been shown that PKC α binds to the cytoplasmic tail of L-selectin (10) and that PKC α activity controls L-selectin shedding in activated T cells (56). It is possible that turnover of the cytoplasmic tail of L-selectin is a mechanism for removing PKC α or other non-receptor kinases and adaptor proteins from the TCR to coordinate TCR signalling for efficient immune cell immunity. Further studies of the proteome in TCR activated T cells where L-selectin processing by ADAM17, PS1 and the proteasome are regulated will be required to fully understand the full impact of L-selectin shedding on T function at sites of immune activity.

Materials and methods

L-selectin expressing T cells

Human L-selectin negative MOLT-3 acute lymphoblastoid T-cells (ATCC CRL-1552) were sequentially transduced to co-express an HIV-1 Gag SLYNTVATL-specific TCR (868) with either human L- V5/His, non-tagged L-selectin or L-selectin-GFP (25) using methods described previously (11). T cells co-expressing 868 TCR and L-selectin were sorted and grown in complete RPMI 1640 medium containing 100 IU penicillin/ml, 100 µg/mL streptomycin, 1 mM sodium pyruvate and supplemented with 10 % FCS (R10). Jurkat cells (ATCC, Clone E6.1) expressing 868 TCR generously provided by John Bridgeman were grown in R10. Mouse embryonic fibroblasts (MEF) deficient in ADAM17 (57) were a kind gift of Carl Blobel (HSS Research Institute, New York) and MEF cells deficient in PS1 and PS2 (PS1/PS2 null) stably expressing exogenous PS1 (+PS1) or PS2 (+ PS2) (23) were a kind gift of B. De Strooper (KUL, Leuven, Belgium). MEF cells were grown in complete DMEM media containing 100 IU penicillin/ml, 100 µg/mL streptomycin, 1 mM sodium pyruvate and supplemented with 10% FCS (D10). For transient transfection, 2.5×10^5 MEF cells/well were seeded in 1 mL D10 in a 24 well plate and grown to 70% confluence at 37 °C for 24 h. Transfection mix containing 8 µL FuGENE 6, 2 µg pcDNA5 expression vector for V5-His tagged wild type human L- selectin and 90 µL Opti-MEM™ medium/well was incubated for 35 min at room temperature, added to MEFs and incubated at 37 °C for 24 h before further experimentation.

L-selectin shedding stimuli

Polyclonal T cell activation using anti-CD3/28: A total of 80 µL Dynabeads™ Human TCR-Activator CD3/CD28 beads (Cat. No 11131D, ThermoFisher) or equivalent numbers of Dynabeads coated with mouse anti-sheep IgG as control (Cat. No 11031, ThermoFisher) were washed in PBS, magnetically pelleted and incubated with 1.3×10^6 MOLT-3 T cells in 100 µL complete RPMI 1640 supplemented with 1 % FCS (R1) for 5 to 60 min in triplicate 96-well U bottomed plates. After TCR-activation, 2.5×10^5 MOLT-3 T cells were prepared for flow cytometry and the remaining MOLT-3 T cells were collected by centrifugation, lysed in RIPA or Laemmli buffer for western blot analysis. Cell-free supernatants were collected for ELISA.

TCR activation by peptide-MHC: TCR-induced L-selectin shedding in MOLT-3 cells was examined in response to HLA-A2⁺ C1R B cells pulsed with cognate SLYNTVATL (SLY) peptide or non-activating NLVPMVATV (NLV) peptide as control (Peptide Synthetics). MOLT-3 cells and C1R cells were rested overnight at 0.9×10^6 cells/ml in RPMI 1640 plus 2 % FCS (R2). The following day, C1R cells were resuspended at 0.5×10^6 cells/ml in the presence of SLY (10^{-7} to 10^{-4} M) or NLV (10^{-5} M) peptides in R2 and plated at 0.5×10^5 cells/well in triplicate in 96-well U-bottomed plates. Cells were incubated for 1h at 37 °C and washed in R2. MOLT-3 cells were resuspended at 1.5×10^6 cells/ml and added to C1R cells at a ratio of 3:1. The plates were incubated for 5-60 min at 37 °C. Cells were washed in ice-cold PBS, pelleted and stained for flow cytometry or lysed for western blot analysis. Cell-free supernatants were stored for ELISA analysis at -20°C. To study the effect of shedding inhibitors, MOLT-3 cells were pre-incubated with D1(A12) for 30 minutes and added to SLY peptide-pulsed C1R cells in R2 containing inhibitors.

Cell activation using PMA: Triplicate wells of MOLT-3 or Jurkat T cells (2.5×10^5 cells/well in 100µl R2 in 96-well U bottomed plates) or MEFs (2.5×10^5 cells/100µl D2 in 24-well plates) were stimulated with 300 nM PMA by addition of 3 µl of 10 µM stock PMA in DMSO) or equivalent amount of DMSO per well and incubated for 15-60 mins at 37°C, 5 % CO₂). Cells were washed in 100 µL ice-cold PBS and stained for flow cytometry or lysed for western blotting.

Inhibitors of L-selectin proteolysis

D1(A12) ADAM17 antibody was obtained from Professor Gillian Murphy (Cambridge University) and used at a concentration of 300 nM and human IgG was used as control. The hydroxamate-based ADAM/MMP metalloproteinase inhibitor Ro 31-9790 was obtained originally from Roche and used at a final concentration of 30 µM. The γ -secretase inhibitors L-685 (5S)-(tert-Butoxycarbonylamino)-6-phenyl-(4R)-hydroxy-(2R)-benzylhexanoyl-L-leucyl-L-phenylalaninamide; Sigma Aldrich) and DAPT (N-[N-(3,5-difluoro-phenacetyl)-L-alanyl]-S-phenylglycine t-butyl ester, ALX-270-416) (Enzo, Life Sciences, Exeter, UK) were both used at 10 µM. Proteasomal inhibitor MG132 (Carbobenzoxy-l-leucyl-l-leucyl-l-leucine) was used at 20µM. MOLT-3 T cells in R1 medium or MEF cells in D1 medium were pre-incubated for 1 h at 37 °C with inhibitors or equivalent levels of DMSO solvent

control at the specified concentrations. L-selectin shedding was stimulated in the presence of the inhibitors or DMSO solvent control as indicated in the figures.

Lysosomal and autophagy inhibitors

Cells were pre-incubated for up to 6 h prior to PMA stimulation with the following inhibitors: bafilomycin A1 which prevents autophagosome-lysosome fusion and deacidifies intracellular compartments (100 nM; Sigma-Aldrich), chloroquine which prevents autophagosome-lysosome fusion (20 μ M; Sigma-Aldrich), leupeptin and pepstatin lysosomal protease inhibitors (both 20 μ M; Sigma-Aldrich) or the autophagy inhibitor MRT68921 (MRT), which inhibits ULK-1 and -2 (1 μ M, Sigma-Aldrich) or DMSO vehicle as control prior to addition of 300 nM PMA in the presence of inhibitors for 30-45 mins.

Analysis of L-selectin proteolysis by western blotting

L-selectin-V5/His positive 1×10^6 MOLT-3 cells and adherent MEFs or Jurkat T cells expressing endogenous (non-V5 tagged) L-selectin were washed in ice-cold PBS and lysed for 30 mins in 35 μ L RIPA buffer (25 mM HEPES at pH 7.4, 150 mM sodium chloride, 10 mM magnesium chloride, 1 mM EDTA, 2 % glycerol, 1 % Triton X-100) supplemented with 4 mM 1,10 phenanthroline, 1 mM sodium orthovanadate, and 1 protease inhibitor tablet per 10 mL of lysis buffer (Roche, Complete protease ULTRA). Cell lysates were centrifuged (5 min, 4 °C, 250 g) and the supernatants were collected and stored at -20 °C or used immediately. In some experiments 1×10^6 MOLT-3 were lysed in 35 μ L Laemmli buffer (660 mM Tris-HCl, pH 6.8, 26 % glycerol (v/v), 4 % SDS (w/v), 0.01 % bromophenol blue (w/v), 5 % β 2-mercaptoethanol (v/v)). Cell lysates were sonicated on ice for 15 sec using a Sonic Dismembrator model-120 (Thermo Scientific) and centrifuged at 13,000 rpm. Collected supernatants were immediately used for SDS-PAGE and western blot analysis. Protein concentrations were determined using the Pierce™ BCA protein assay (ThermoFisher).

Lysates were mixed with equal volume of Laemmli sample buffer, heat denatured and loaded onto 4-10% gradient gels (Bio-Rad) and resolved at 100 V. Proteins were transferred to activated PVDF Transfer Membrane (methanol, 30s, RT) with a pore size of 0.2 μ m (Thermo Fisher Scientific; 88520)

for the capture of small proteins using the X-cell module (60 min, 30 V) according to the manufacturer's protocol with NuPage transfer buffer (Thermo Fisher Scientific; NP0006).

Membranes were blocked with 5% milk powder in PBS/0.1 % Tween 20 (PBS-T) for 1h at RT prior to incubation with mouse monoclonal anti-V5 (R960-25, Invitrogen; 1 in 1000) or CA21 L-selectin cyto tail antibody (Boehringer-Ingelheim; 1/400) {Kahn, 1998 #32}; overnight at 4°C with rocking. The following day, the PVDF membrane was washed 5x in PBS-T (5 min, RT, rocking) before addition of the secondary horseradish peroxidase (HRP) -conjugated antibody (Bio-Rad; 1706516; 1.6/1000 in 5 % milk PBS-T; 60 min, RT, rocking). The PVDF membrane was washed 5x in PBS-T (5 min, RT, rocking) before development of the membrane using a chemiluminescent substrate (Thermo Fisher Scientific; 34580) and imaged using a Syngene G:Box or iBright 1500. Following imaging, PVDF membranes were stripped according to manufacturer's protocol (Thermo Fisher Scientific, 21059; 15 min, 37 °C) before washing 5x in PBS-T (5 min, RT, rocking), blocking with 5 % milk in PBS-T and re-probing for GAPDH using anti-GAPDH (Abcam, ab9484, 0.32/1000) as primary antibody. For long-term storage, PVDF membranes were sealed in bags with PBS-T.

Conventional Flow cytometry

For surface staining, cells were washed in PBS 2 % FCS, labelled with Live/Dead Fixable Aqua (Life Technologies), washed in PBS 2 % FCS, and blocked with PBS 2% FCS containing 5 % rat serum. Cells were stained with relevant antibodies for 30 minutes at 4–8 °C, washed in PBS 2 % FCS, fixed with 4 % paraformaldehyde, and resuspended after a wash in 200 µl PBS 2 % FCS. Cells were analysed on a BD FACSCanto II machine using DIVA software and data analysed using FlowJo V10. UltraComp eBeads (ThermoFisher) were used following manufacturer's protocols for compensation during flow cytometry analysis. T cells were stained using anti-CD62L-PE (DREG56) with isotype control P3.6.2.8.1-PE (IgG1κ) (eBioscience). T cell-APC mixtures were co-stained for CD19 using anti-CD19-APC (H1B18) (BD Biosciences) with isotype control 11711-APC (IgG1κ) (R & D Systems) and CD62L on CD19 negative MOLT-3 T cells analysed. Cell surface L-selectin expression on MOLT-3 T cells was calculated relative to non-TCR stimulated cells after subtracting median fluorescence intensity or % positive cells for isotype control Ab stained cells from all samples:

% cell surface L-selectin = $100 \times (\text{MFI of TCR activated T cells} - \text{MFI isotype control}) / (\text{MFI unactivated T cells} - \text{MFI isotype control})$

Imaging Flow Cytometry

T cells were surface stained as for conventional flow cytometry, washed once in PBS prior to fixation in 2 % fresh formaldehyde (2 % v/v in PBS; 60 mins, RT; Pierce; 28906). Following this, cells were washed three times in 200 μL True Nuclear permeabilisation buffer (BioLegend; 424401) before staining with 50 μL of diluted antibody (again in permeabilisation buffer; 30 min, RT). Cells were then washed three times in 200 μL True Nuclear permeabilisation buffer. For nuclear staining, cells were centrifuged (5 min, 4 $^{\circ}\text{C}$, 1200 rpm) and 15 μL NucBlue (Invitrogen; R37605) was added to each sample (20 min, RT). Otherwise, cells were resuspended in 15 μL FACS buffer. T cells were stained with the following antibodies: CD62L-APC/Fire 750 (DREG56, IgG1 κ ; BioLegend), CD69-PE (FN50, IgG1 κ ; Biolegend), V5-AF647 (AB2532221, IgG2a; Invitrogen) and CD107a-FITC (H4A3, IgG1 κ Invitrogen). Prior to analysis, cells were transferred to eppendorf tubes, wrapped in foil and stored (4 $^{\circ}\text{C}$) until analysis. Data acquisition was conducted at a 60x magnification using an ImageStream X Mark II imaging flow cytometer. During acquisition singlets were exported for data analysis. Controls for ImageStream analysis were created through single stains of each antibody and relevant isotypes on live cells and following incubation at 95 $^{\circ}\text{C}$ for 5 mins for LIVE/DEAD stain. Analysis was performed using IDEAS software. The imaging flow cytometry software package uses a log-transformed Pearson's correlation co-efficient to evaluate the similarity in the distribution of fluorescence between two probes within user-defined sub-cellular compartments or 'masks'. The software reports this as a 'similarity score'. The spot counting feature within IDEAS software was used to distinguish bright regions of a cell from background fluorescence using a user-defined spot-to-cell background in user-defined masks.

Soluble L-selectin

Soluble L-selectin was quantitated by ELISA (Human L-selectin/CD62L DuoSet ELISA, DY728, R & D systems) according to manufacturer's instructions and absorbance measured immediately at 450 nM using a Clariostat microplate reader. The detection limit was 0.078 ng/ml.

Statistical analysis

All statistical analyses were conducted using GraphPad PRISM 10.0.3. Data were tested for normality using the Shapiro-Wilk test. Statistical tests used are presented in each figure legend. P-values < 0.05 were deemed significant. In each graph or plot, either the individual values and mean are shown, or the mean and standard deviation. Fisher's least significant difference test is abbreviated in figure legends as Fisher's LSD. Each experiment contains data from 3 independent experiments (n=3).

Journal Pre-proof

Supporting Information

This article contains supporting information.

Acknowledgements

We thank Carl Blobel for providing ADAM17-deficient MEFs, Bart de Strooper for providing PS1/2-deficient MEFs, Stephen Cobbold for advice on defining cell membrane masks for analysis of Imaging Flow Cytometry data, and Miriam Vigar for technical assistance. We thank Dr Michael May for critical appraisal of the study.

Author contributions

VK and AA conceived the study. ORM, ACN, ASA, SCW, and KB-G performed the experiments. VK and AA supervised the study with critical input from AI and DAP. ORM, ACN, VK, and AA wrote the manuscript with contributions from all authors.

Funding sources

This work was supported by PhD studentships from Cardiff University (ORM), the Medical Research Council (ACN, SCW), and the Saudi Arabian Cultural Bureau, London (ASA), and by a Biotechnology and Biological Sciences Research Council grant awarded to VK and AA (BB/S002480/1). KB-G was supported by the Socrates ERASMUS Program. DAP was supported by a Wellcome Trust Senior Investigator Award (100326/Z/12/Z). AI was supported by BHF Centre of Research Excellence at King's College London: RE/13/2/30182. The iBright 1500 was supported by Sêr Cymru II with matched funding from Cardiff University and the European Regional Development Fund via the Welsh Government (CU209 to VK and Manon Pritchard).

Conflicts

The authors declare that the research was conducted in the absence of any commercial or financial relationships that could be construed as a potential conflict of interest.

Consent statement

Consent was not required for this study.

References

1. Ley, K., Laudanna, C., Cybulsky, M. I., and Nourshargh, S. (2007) Getting to the site of inflammation: the leukocyte adhesion cascade updated. *Nature Reviews Immunology* **7**, 678-689
2. Rosen, S. D. (2004) Ligands for L-selectin: Homing, inflammation, and beyond. *Annual review of immunology* **22**, 129-156
3. Nishijima, K., Ando, M., Sano, S., Hayashi-Ozawa, A., Kinoshita, Y., and Iijima, S. (2005) Costimulation of T-cell proliferation by anti-L-selectin antibody is associated with the reduction of a cdk inhibitor p27. *Immunology* **116**, 347-353
4. Brenner, B., Gulbins, E., Schlottmann, K., Koppenhoefer, U., Busch, G. L., Walzog, B., Steinhausen, M., Coggeshall, K. M., Linderkamp, O., and Lang, F. (1996) L-selectin activates the Ras pathway via the tyrosine kinase p56lck. *Proceedings of the National Academy of Sciences of the United States of America* **93**, 15376-15381
5. Chen, C., Shang, X., Xu, T., Cui, L., Luo, J., Ba, X., Hao, S., and Zeng, X. (2007) c-Abl is required for the signaling transduction induced by L-selectin ligation. *European journal of immunology* **37**, 3246-3258
6. Seth, A., Gote, L., Nagarkatti, M., and Nagarkatti, P. S. (1991) T-cell-receptor-independent activation of cytolytic activity of cytotoxic T lymphocytes mediated through CD44 and gp90MEL-14. *Proc Natl Acad Sci U S A* **88**, 7877-7881
7. Brenner, B., Gulbins, E., Busch, G. L., Koppenhoefer, U., Lang, F., and Linderkamp, O. (1997) L-selectin regulates actin polymerisation via activation of the small G-protein Rac2. *Biochem Biophys Res Commun* **231**, 802-807
8. Hwang, S. T., Singer, M. S., Giblin, P. A., Yednock, T. A., Bacon, K. B., Simon, S. I., and Rosen, S. D. (1996) GlyCAM-1, a physiologic ligand for L-selectin, activates beta 2 integrins on naive peripheral lymphocytes. *J Exp Med* **184**, 1343-1348
9. Giblin, P. A., Hwang, S. T., Katsumoto, T. R., and Rosen, S. D. (1997) Ligation of L-selectin on T lymphocytes activates beta1 integrins and promotes adhesion to fibronectin. *J Immunol* **159**, 3498-3507
10. Kilian, K., Denedde, J., Mueller, E. C., Bahr, I., and Tauber, R. (2004) The interaction of protein kinase C isozymes alpha, iota, and theta with the cytoplasmic domain of L-selectin is modulated by phosphorylation of the receptor. *The Journal of biological chemistry* **279**, 34472-34480
11. Mohammed, R. N., Wehenkel, S. C., Galkina, E. V., Yates, E.-K., Preece, G., Newman, A., Watson, H. A., Ohme, J., Bridgeman, J. S., Durairaj, R. R. P., Moon, O. R., Ladell, K., Miners, K. L., Dolton, G., Troeberg, L., Kashiwagi, M., Murphy, G., Nagase, H., Price, D. A., Matthews, R. J., Knäuper, V., and Ager, A. (2019) ADAM17-dependent proteolysis of L-selectin promotes early clonal expansion of cytotoxic T cells. *Scientific Reports* **9**, 5487
12. Richards, H., Longhi, M. P., Wright, K., Gallimore, A., and Ager, A. (2008) CD62L (L-Selectin) Down-Regulation Does Not Affect Memory T Cell Distribution but Failure to Shed Compromises Anti-Viral Immunity. *J Immunol* **180**, 198-206
13. Watson, H. A., Durairaj, R. R. P., Ohme, J., Alatsatianos, M., Almutairi, H., Mohammed, R. N., Vigar, M., Reed, S. G., Paisey, S. J., Marshall, C., Gallimore, A., and Ager, A. (2019) L-selectin enhanced T cells improve the efficacy of cancer immunotherapy. *Frontiers in immunology* **10**, 1321-1321
14. Yang, S., Liu, F., Wang, Q. J., Rosenberg, S. A., and Morgan, R. A. (2011) The Shedding of CD62L (L-Selectin) Regulates the Acquisition of Lytic Activity in Human Tumor Reactive T Lymphocytes. *PLOS ONE* **6**, e22560
15. Tape, C. J., Willems, S. H., Dombernowsky, S. L., Stanley, P. L., Fogarasi, M., Ouwehand, W., McCafferty, J., and Murphy, G. (2011) Cross-domain inhibition of TACE ectodomain. *Proc Natl Acad Sci U S A* **108**, 5578-5583
16. Struhl, G., and Adachi, A. (2000) Requirements for presenilin-dependent cleavage of notch and other transmembrane proteins. *Mol Cell* **6**, 625-636
17. Murphy, G., Murthy, A., and Khokha, R. (2008) Clipping, shedding and RIPping keep immunity on cue. *Trends Immunol* **29**, 75-82
18. Shearman, M. S., Beher, D., Clarke, E. E., Lewis, H. D., Harrison, T., Hunt, P., Nadin, A., Smith, A. L., Stevenson, G., and Castro, J. L. (2000) L-685,458, an aspartyl protease

- transition state mimic, is a potent inhibitor of amyloid beta-protein precursor gamma-secretase activity. *Biochemistry* **39**, 8698-8704
19. Dovey, H. F., John, V., Anderson, J. P., Chen, L. Z., de Saint Andrieu, P., Fang, L. Y., Freedman, S. B., Folmer, B., Goldbach, E., Holsztynska, E. J., Hu, K. L., Johnson-Wood, K. L., Kennedy, S. L., Kholodenko, D., Knops, J. E., Latimer, L. H., Lee, M., Liao, Z., Lieberburg, I. M., Motter, R. N., Mutter, L. C., Nietz, J., Quinn, K. P., Sacchi, K. L., Seubert, P. A., Shopp, G. M., Thorsett, E. D., Tung, J. S., Wu, J., Yang, S., Yin, C. T., Schenk, D. B., May, P. C., Altstiel, L. D., Bender, M. H., Boggs, L. N., Britton, T. C., Clemens, J. C., Czilli, D. L., Dieckman-McGinty, D. K., Droste, J. J., Fuson, K. S., Gitter, B. D., Hyslop, P. A., Johnstone, E. M., Li, W. Y., Little, S. P., Mabry, T. E., Miller, F. D., and Audia, J. E. (2001) Functional gamma-secretase inhibitors reduce beta-amyloid peptide levels in brain. *J Neurochem* **76**, 173-181
 20. Li, N., Wang, Y., Forbes, K., Vignali, K. M., Heale, B. S., Saftig, P., Hartmann, D., Black, R. A., Rossi, J. J., Blobel, C. P., Dempsey, P. J., Workman, C. J., and Vignali, D. A. (2007) Metalloproteases regulate T-cell proliferation and effector function via LAG-3. *The EMBO journal* **26**, 494-504
 21. Le Gall, S. M., Bobe, P., Reiss, K., Horiuchi, K., Niu, X. D., Lundell, D., Gibb, D. R., Conrad, D., Saftig, P., and Blobel, C. P. (2009) ADAMs 10 and 17 represent differentially regulated components of a general shedding machinery for membrane proteins such as transforming growth factor alpha, L-selectin, and tumor necrosis factor alpha. *Mol Biol Cell* **20**, 1785-1794
 22. De Strooper, B., Annaert, W., Cupers, P., Saftig, P., Craessaerts, K., Mumm, J. S., Schroeter, E. H., Schrijvers, V., Wolfe, M. S., Ray, W. J., Goate, A., and Kopan, R. (1999) A presenilin-1-dependent gamma-secretase-like protease mediates release of Notch intracellular domain. *Nature* **398**, 518-522
 23. Herreman, A., Serneels, L., Annaert, W., Collen, D., Schoonjans, L., and De Strooper, B. (2000) Total inactivation of gamma-secretase activity in presenilin-deficient embryonic stem cells. *Nat Cell Biol* **2**, 461-462
 24. Owens, H. A., Thorburn, L. E., Walsby, E., Moon, O. R., Rizkallah, P., Sherwani, S., Tinsley, C. L., Rogers, L., Cerutti, C., Ridley, A. J., Williams, J., Knauper, V., and Ager, A. (2024) Alzheimer's disease-associated P460L variant of EphA1 dysregulates receptor activity and blood-brain barrier function. *Alzheimers Dement* **20**, 2016-2033
 25. Rzeniewicz, K., Neue, A., Rey Gallardo, A., Davies, J., Holt, M. R., Patel, A., Charras, G. T., Stramer, B., Molenaar, C., Tedder, T. F., Parsons, M., and Ivetic, A. (2015) L-selectin shedding is activated specifically within transmigrating pseudopods of monocytes to regulate cell polarity in vitro. *Proc Natl Acad Sci U S A* **112**, E1461-1470
 26. Gifford, J. L., Ishida, H., and Vogel, H. J. (2012) Structural insights into calmodulin-regulated L-selectin ectodomain shedding. *The Journal of biological chemistry* **287**, 26513-26527
 27. Kahn, J., Walcheck, B., Migaki, G. I., Jutila, M. A., and Kishimoto, T. K. (1998) Calmodulin regulates L-selectin adhesion molecule expression and function through a protease-dependent mechanism. *Cell* **92**, 809-818
 28. Ivetic, A., Deka, J., Ridley, A., and Ager, A. (2002) The cytoplasmic tail of L-selectin interacts with members of the Ezrin-Radixin-Moesin (ERM) family of proteins: cell activation-dependent binding of Moesin but not Ezrin. *The Journal of biological chemistry* **277**, 2321-2329
 29. Ivetic, A., Florey, O., Deka, J., Haskard, D. O., Ager, A., and Ridley, A. J. (2004) Mutagenesis of the ezrin-radixin-moesin binding domain of L-selectin tail affects shedding, microvillar positioning, and leukocyte tethering. *The Journal of biological chemistry* **279**, 33263-33272
 30. Kimberly, W. T., LaVoie, M. J., Ostaszewski, B. L., Ye, W., Wolfe, M. S., and Selkoe, D. J. (2003) Gamma-secretase is a membrane protein complex comprised of presenilin, nicastrin, Aph-1, and Pen-2. *Proc Natl Acad Sci U S A* **100**, 6382-6387
 31. Thinakaran, G., Teplow, D. B., Siman, R., Greenberg, B., and Sisodia, S. S. (1996) Metabolism of the "Swedish" amyloid precursor protein variant in neuro2a (N2a) cells. Evidence that cleavage at the "beta-secretase" site occurs in the golgi apparatus. *The Journal of biological chemistry* **271**, 9390-9397

32. Podlisny, M. B., Citron, M., Amarante, P., Sherrington, R., Xia, W., Zhang, J., Diehl, T., Levesque, G., Fraser, P., Haass, C., Koo, E. H., Seubert, P., St George-Hyslop, P., Teplow, D. B., and Selkoe, D. J. (1997) Presenilin proteins undergo heterogeneous endoproteolysis between Thr291 and Ala299 and occur as stable N- and C-terminal fragments in normal and Alzheimer brain tissue. *Neurobiol Dis* **3**, 325-337
33. Steiner, H., Duff, K., Capell, A., Romig, H., Grim, M. G., Lincoln, S., Hardy, J., Yu, X., Picciano, M., Fichtler, K., Citron, M., Kopan, R., Pesold, B., Keck, S., Baader, M., Tomita, T., Iwatsubo, T., Baumeister, R., and Haass, C. (1999) A loss of function mutation of presenilin-2 interferes with amyloid beta-peptide production and notch signaling. *The Journal of biological chemistry* **274**, 28669-28673
34. De Strooper, B., Saftig, P., Craessaerts, K., Vanderstichele, H., Guhde, G., Annaert, W., Von Figura, K., and Van Leuven, F. (1998) Deficiency of presenilin-1 inhibits the normal cleavage of amyloid precursor protein. *Nature* **391**, 387-390
35. Fiaturi, N., Ritzkat, A., Dammann, C. E., Castellot, J. J., and Nielsen, H. C. (2014) Dissociated presenilin-1 and TACE processing of ErbB4 in lung alveolar type II cell differentiation. *Biochim Biophys Acta* **1843**, 797-805
36. Fryer, C. J., White, J. B., and Jones, K. A. (2004) Mastermind recruits CycC:CDK8 to phosphorylate the Notch ICD and coordinate activation with turnover. *Mol Cell* **16**, 509-520
37. May, P., Reddy, Y. K., and Herz, J. (2002) Proteolytic processing of low density lipoprotein receptor-related protein mediates regulated release of its intracellular domain. *The Journal of biological chemistry* **277**, 18736-18743
38. Liu, C. X., Ranganathan, S., Robinson, S., and Strickland, D. K. (2007) gamma-Secretase-mediated release of the low density lipoprotein receptor-related protein 1B intracellular domain suppresses anchorage-independent growth of neuroglioma cells. *The Journal of biological chemistry* **282**, 7504-7511
39. Carey, B. W., Kim, D. Y., and Kovacs, D. M. (2007) Presenilin/gamma-secretase and alpha-secretase-like peptidases cleave human MHC Class I proteins. *Biochem J* **401**, 121-127
40. Haas, I. G., Frank, M., Veron, N., and Kemler, R. (2005) Presenilin-dependent processing and nuclear function of gamma-protocadherins. *The Journal of biological chemistry* **280**, 9313-9319
41. Cupers, P., Orleans, I., Craessaerts, K., Annaert, W., and De Strooper, B. (2001) The amyloid precursor protein (APP)-cytoplasmic fragment generated by gamma-secretase is rapidly degraded but distributes partially in a nuclear fraction of neurones in culture. *J Neurochem* **78**, 1168-1178
42. Edbauer, D., Willem, M., Lammich, S., Steiner, H., and Haass, C. (2002) Insulin-degrading enzyme rapidly removes the beta-amyloid precursor protein intracellular domain (AICD). *The Journal of biological chemistry* **277**, 13389-13393
43. Cao, X., and Sudhof, T. C. (2001) A transcriptionally [correction of transcriptively] active complex of APP with Fe65 and histone acetyltransferase Tip60. *Science* **293**, 115-120
44. von Rotz, R. C., Kohli, B. M., Bosset, J., Meier, M., Suzuki, T., Nitsch, R. M., and Konietzko, U. (2004) The APP intracellular domain forms nuclear multiprotein complexes and regulates the transcription of its own precursor. *J Cell Sci* **117**, 4435-4448
45. Schroeter, E. H., Kisslinger, J. A., and Kopan, R. (1998) Notch-1 signalling requires ligand-induced proteolytic release of intracellular domain. *Nature* **393**, 382-386
46. Oberg, C., Li, J., Pauley, A., Wolf, E., Gurney, M., and Lendahl, U. (2001) The Notch intracellular domain is ubiquitinated and negatively regulated by the mammalian Sel-10 homolog. *The Journal of biological chemistry* **276**, 35847-35853
47. Gupta-Rossi, N., Le Bail, O., Gonen, H., Brou, C., Logeat, F., Six, E., Ciechanover, A., and Israel, A. (2001) Functional interaction between SEL-10, an F-box protein, and the nuclear form of activated Notch1 receptor. *The Journal of biological chemistry* **276**, 34371-34378
48. Lange, A., Mills, R. E., Devine, S. E., and Corbett, A. H. (2008) A PY-NLS nuclear targeting signal is required for nuclear localization and function of the *Saccharomyces cerevisiae* mRNA-binding protein Hrp1. *The Journal of biological chemistry* **283**, 12926-12934
49. Wolf, T., Jin, W., Zoppi, G., Vogel, I. A., Akhmedov, M., Bleck, C. K. E., Beltraminelli, T., Rieckmann, J. C., Ramirez, N. J., Benevento, M., Notarbartolo, S., Bumann, D., Meissner, F., Grimbacher, B., Mann, M., Lanzavecchia, A., Sallusto, F., Kwee, I., and Geiger, R.

- (2020) Dynamics in protein translation sustaining T cell preparedness. *Nat Immunol* **21**, 927-937
50. Coscoy, L., and Ganem, D. (2000) Kaposi's sarcoma-associated herpesvirus encodes two proteins that block cell surface display of MHC class I chains by enhancing their endocytosis. *Proc Natl Acad Sci U S A* **97**, 8051-8056
51. Hewitt, E. W., Duncan, L., Mufti, D., Baker, J., Stevenson, P. G., and Lehner, P. J. (2002) Ubiquitylation of MHC class I by the K3 viral protein signals internalization and TSG101-dependent degradation. *The EMBO journal* **21**, 2418-2429
52. Timms, R. T., Mena, E. L., Leng, Y., Li, M. Z., Tchasovnikarova, I. A., Koren, I., and Elledge, S. J. (2023) Defining E3 ligase-substrate relationships through multiplex CRISPR screening. *Nat Cell Biol* **25**, 1535-1545
53. Mohammed, R. N., Watson, H. A., Vigar, M., Ohme, J., Thomson, A., Humphreys, I. R., and Ager, A. (2016) L-selectin Is Essential for Delivery of Activated CD8(+) T Cells to Virus-Infected Organs for Protective Immunity. *Cell reports* **14**, 760-771
54. Galkina, E., Tanousis, K., Preece, G., Tolaini, M., Kioussis, D., Florey, O., Haskard, D. O., Tedder, T. F., and Ager, A. (2003) L-selectin shedding does not regulate constitutive T cell trafficking but controls the migration pathways of antigen-activated T lymphocytes. *Journal of Experimental Medicine*. **198**, 1323-1335
55. Jung, Y., Riven, I., Feigelson, S. W., Kartvelishvily, E., Tohya, K., Miyasaka, M., Alon, R., and Haran, G. (2016) Three-dimensional localization of T-cell receptors in relation to microvilli using a combination of superresolution microscopies. *Proc Natl Acad Sci U S A* **113**, E5916-E5924
56. Gharbi, S. I., Avila-Flores, A., Soutar, D., Orive, A., Koretzky, G. A., Albar, J. P., and Merida, I. (2013) Transient PKCalpha shuttling to the immunological synapse is governed by DGKzeta and regulates L-selectin shedding. *J Cell Sci* **126**, 2176-2186
57. Reddy, P., Slack, J. L., Davis, R., Cerretti, D. P., Kozlosky, C. J., Blanton, R. A., Shows, D., Peschon, J. J., and Black, R. A. (2000) Functional analysis of the domain structure of tumor necrosis factor-alpha converting enzyme. *The Journal of biological chemistry* **275**, 14608-14614

Figure 1: L-selectin ectodomain shedding is mediated by ADAM-17 irrespective of the mode of T cell activation and intracellular domain tag.

(A) Schematic representation of L-selectin expression constructs used in this study (GFP, green fluorescent protein). (B) 868 TCR+ MOLT-3 cells expressing either wild type (CD62L) or V5/His tagged (CD62L-V5) L-selectin were either pretreated with the metalloproteinase inhibitor Ro 31-9790 or DMSO solvent control prior to engaging the 868 TCR with SLY peptide primed antigen presenting cells at the indicated concentrations. Data show percentage of cells expressing cell surface L-selectin measured by flow cytometry (mean \pm SD, n=3). Gating strategy shown in Fig. S1. (C) Western blot analysis of 868 TCR+ MOLT-3 cells pretreated with either an inhibitory ADAM 17 antibody or hIgG control antibody and stimulated with T cell activator beads. Bands for full length L-selectin-V5/His and the membrane retained L-selectin-V5/His fragment (MRF) are indicated. (D) Flow cytometric analysis of cell surface L-selectin following T cell activation with either PMA or SLY-pulsed antigen presenting cells in the presence or absence of inhibitory ADAM17 antibody.

Figure 2: L-selectin ectodomain proteolysis by ADAM-17 is not prevented by gamma-secretase inhibition.

(A-C) 868 TCR+ MOLT-3 cells expressing V5/His tagged L-selectin (CD62L-V5) were either pretreated with the γ -secretase inhibitor L-685 or DMSO solvent control prior to stimulation with either T cell activator or control beads for the indicated times. Representative histograms showing cell surface expression of L-selectin (A), frequency of L-selectin positive cells (B) and soluble L-selectin (C) are shown. Data are means \pm SD, n = 3. (D-F). 868 TCR+ MOLT-3 cells expressing V5/His tagged L-selectin (CD62L-V5) were either pretreated with the γ -secretase inhibitor L-685 or blocking ADAM17 antibody and relevant controls prior to stimulation PMA or solvent control. Representative histograms showing cell surface expression of L-selectin (E), frequency of L-selectin positive cells. Data are means \pm SD, n = 3. Two-way ANOVA with Fisher's LSD test.

Figure 3: The membrane retained fragment of L-selectin is produced by ADAM-17 ectodomain shedding and is degraded by gamma-secretase.

868 TCR+ MOLT-3 cells expressing V5/His tagged L-selectin (CD62L-V5) were either pretreated with the protease inhibitors or solvent control prior to stimulation of ADAM17 with T cell activator or control beads or PMA for the indicated times and analysed by western blotting. Representative blots of lysates from control (A), T cell activated (B) and T cell activated in the presence of γ -secretase inhibitor (C). Bands for full length L-selectin-V5/His and the membrane retained L-selectin-V5/His fragment (MRF) are indicated. Histograms show Fold change in full length L-selectin in control (D), T cell activated (E) and T cell activated in the presence of γ -secretase inhibitor (F) and fold change in MRF for T cell activated (G) and T cell activated in the presence of γ -secretase inhibitor (H). Representative blots of lysates from control and PMA activated cells in the presence of γ -secretase or ADAM17 inhibitor (I). Histograms show Fold change in MRF for PMA activated cells (J). Data shown means \pm SD, n=3. (D-H) One-way ANOVA with post-hoc Tukey test. (J) Two way ANOVA with Fisher's LSD test.

Figure 4. PS1 mediates intramembrane proteolysis of the ADAM17 product of L-selectin.

(A, B) PS1 and PS2 isoform expression in WT, PS1/2 double knockout (PS1/2 null) and PS1/2 null cells expressing PS1 (+PS1) or PS2 (+PS2) validated by immunoblotting. (C, D) WT or PS1/2 double knockout (PS1/2 null) MEF cells were transiently transfected with L-selectin-V5/His, incubated with L-685 or Ro 31-9790 or DMSO solvent control and analysed by western blotting. Representative blots (C) and fold changes in MRF in the presence of L-685 and Ro 31-9790 are shown (D). (E, F) PS1/2 null MEF cells complimented with PS1 (+ PS1) or PS2 (+ PS2) were transiently transfected with L-selectin-V5/His and incubated with DMSO, L-685 or Ro 31-9790. Representative blots (E) and fold changes in MRF in the presence of L-685 and Ro 31-9790 (F) are shown. Results are mean of three independent experiments (n=3), \pm SD. One-way ANOVA with post-hoc Tukey test.

Figure 5. L-selectin intracellular domain proteolysis by gamma-secretase causes release from the membrane.

868 TCR+ MOLT-3 cells expressing V5/His tagged L-selectin (CD62L-V5) were either pretreated with L-685 or solvent control prior to stimulation of ADAM17 with PMA for 15 min. Live cells were stained for CD69 (membrane), fixed and permeabilised and then stained for V5 (CD62L tail), CD107a (lysosome) and NucBlue (nucleus) and analysed by imaging flow cytometry. Triple positive events were AND-gated and assessed for similarity scores between CD62L-V5 and CD69 (membrane), CD62L-V5 and CD107a (lysosome) and CD62L-V5 and NucBlue (nucleus). (A) Representative NucBlue, CD107a, CD69 and CD62L-V5 staining of a single cell and cell masks used to assess similarity scores. (B-D) Representative overlay histograms of similarity scores for L-selectin-V5 tag in the membrane (B), lysosome (C) and nuclear (D) compartments of control (DMSO, black unshaded) and activated (PMA, green shaded) cells. Black arrow in B indicate shift induced by PMA. (E-G) Representative overlay histograms of similarity scores for L-selectin cyto tail in the membrane (E), lysosome (F) and nuclear (G) compartments of L-685 pretreated control (DMSO, black unshaded) and activated (PMA, cyan shaded) cells. White arrow in E shows no shift induced by PMA in the presence of L-685. (H-J) Replicate median similarity scores in response to PMA in the absence and presence of γ -secretase inhibitor L-685 in membrane (H), lysosomal (I) and nuclear (J) compartments. Data show mean similarity scores for each replicate without (black symbols) and with PMA (green symbols), n=3. Two-way ANOVA with Fishers's LSD test.

Figure 6. L-selectin intracellular domain proteolysis by gamma-secretase causes release from the membrane and degradation.

MOLT-3 cells expressing CD62L-GFP (A-E) were incubated with PMA or DMSO solvent control for 15 min and stained for membrane CD69. CD69 and GFP were analysed by imaging flow cytometry in live cells and following fixation and permeabilization. (A-D). Representative overlay histograms showing whole cell L-selectin-GFP or CD69 fluorescence signals in the presence (green shaded) and absence (black unshaded) of PMA in live (A, B) and fixed/permeabilised cells (C, D). Black arrows in A and C indicate shifts induced by PMA. (E) Median fluorescence whole cell intensities of

GFP in response to PMA in replicate experiments. Results show data points and bars show means \pm SD, n = 6. One-way ANOVA with Tukeys multiple comparisons test. (F) 868 TCR+ MOLT-3 cells expressing CD62L-V5 were incubated with PMA or DMSO solvent control for 15 min and live, focussed, single cells analysed for whole cell median fluorescence intensity of L-selectin cyto tail using V5 staining. Data points show median fluorescence whole cell intensities of V5 in response to PMA. Bars represent means \pm SD, n = 6. Unpaired t test. (G) Fold change in CD62L cytotail (GFP or V5) whole cell intensities in response to PMA. Results show data points and bars show means \pm SD, n = 6. One-way ANOVA with Tukey's multiple comparisons test. ns, not significant.

Figure 7. The membrane retained fragment of CD62L generated by TCR activation is degraded by γ -secretase and proteasome

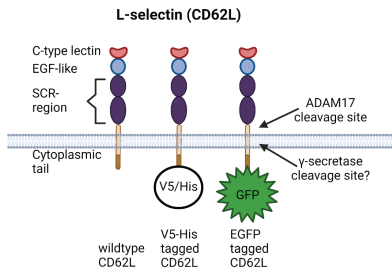
868 TCR+ MOLT-3 cells expressing CD62L-V5 were pretreated with the indicated protease inhibitors or solvent control prior to activation by SLY or NLV peptide pulsed antigen presenting cells (A-C) or PMA (D-F). Cells were lysed and immunoblotted for L-selectin's V5/His tagged cytosolic tail and GAPDH as a control for protein loading. (A) A representative western blot for full-length CD62L-V5/His and MRF and GAPDH as loading control. (B) Quantification of full-length L-selectin relative to GAPDH control and presentation as fold change following peptide treatment. (C) Quantification of MRF relative to GAPDH control and presentation as fold change following Peptide treatment. (D) A representative western blot for full-length and L-selectin tail containing MRF fragment following pretreatment with the indicated lysosomal and autophagy inhibitors prior to incubation with PMA. Results show Fold change in L-selectin MRF fragment in the absence (E) and presence of PMA (F). Results are mean of three independent experiments (n=3), \pm SD. One-way ANOVA with Tukey's multiple comparisons test. Lysosomal inhibitors: BAF, bafilomyin; ChQ, chloroquine; P + L, pepstatin and leupeptin. Autophagy inhibitor: MRF, MRT68921.

Figure 8. TCR activation stimulates regulated intramembrane proteolysis of cell surface L-selectin by presenilin 1 and localised proteasomal degradation of the cytoplasmic tail

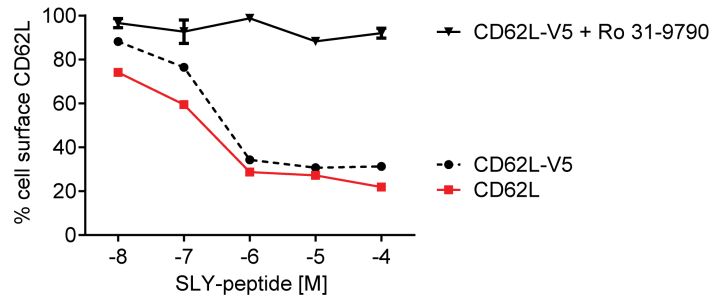
Based on a combination of imaging and biochemical experiments using genetic manipulation and pharmacological inhibitors, we propose that cell surface L-selectin undergoes the following sequence of processing steps in T cells following engagement of the TCR. (1) Protein kinase C dependent proteolysis of L-selectin ectodomain (CD62L-ECD) by ADAM17 and release of C62L-ECD from the T cell surface. (2) The membrane retained fragment (CD62L-MRF) generated by ADAM17 forms a complex with γ -secretase and undergoes intramembrane cleavage by the PS1 subunit of γ -secretase. (3) The cytoplasmic tail (CD62L-ICD) generated by PS1 undergoes proteasomal degradation. The CD62L-MRF was not translocated to (4) the nucleus for downstream signalling, (5) the lysosome for degradation or (6) the autophagosome for recycling. Proteasomal degradation of L-selectin cytoplasmic tail occurred within 15 mins of T cell activation.

Figure 1

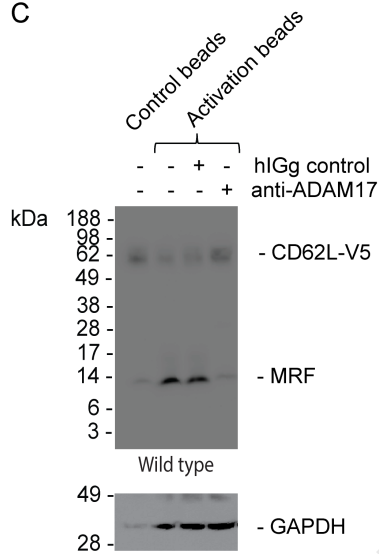
A



B



C



D

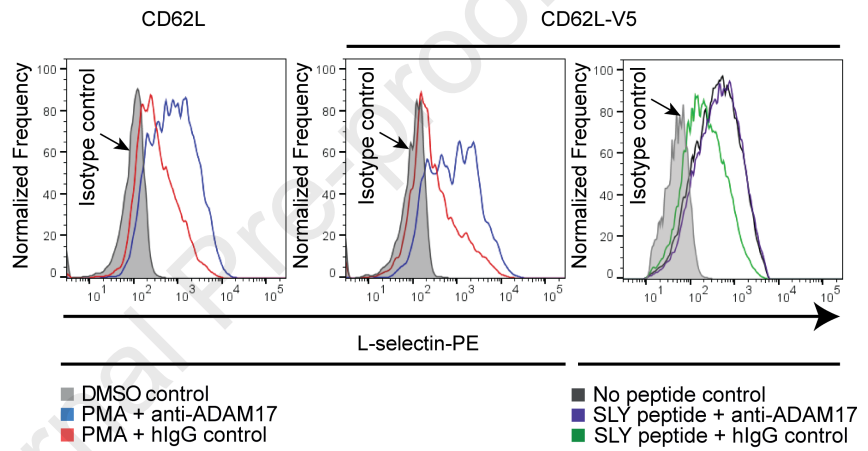
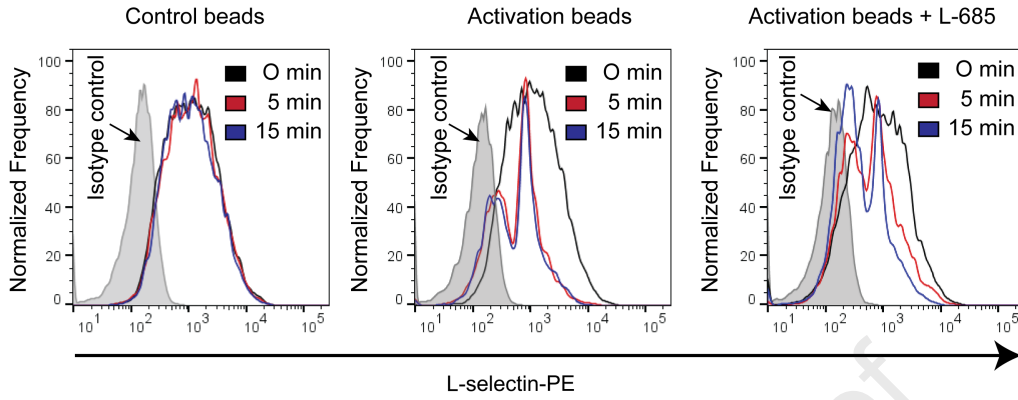
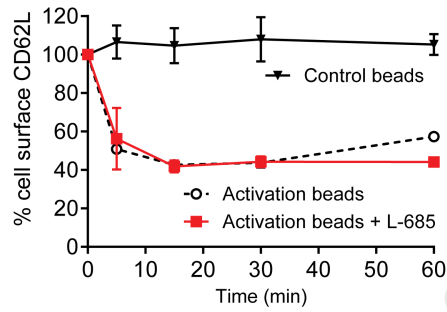


Figure 2

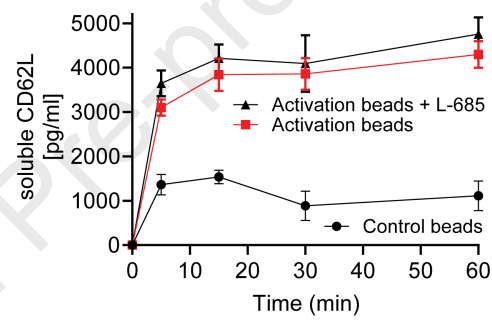
A



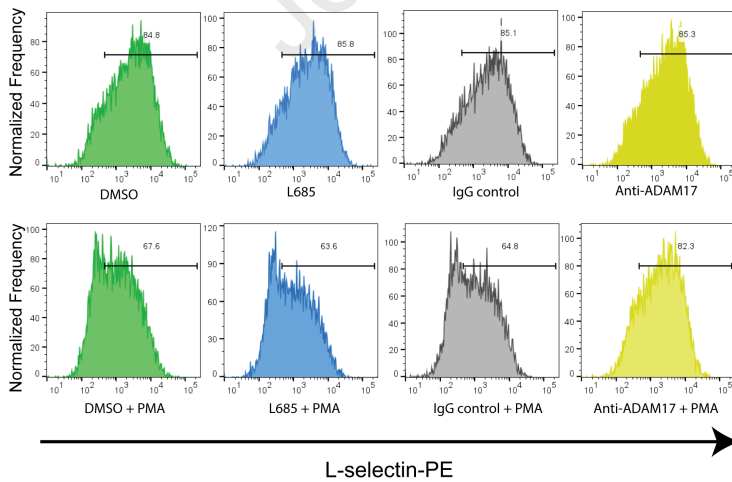
B



C



D



E

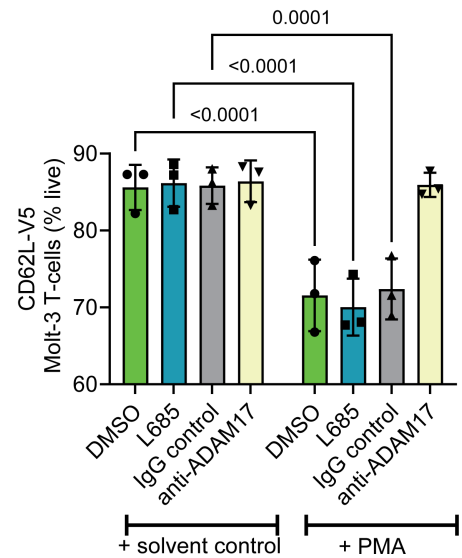


Figure 3

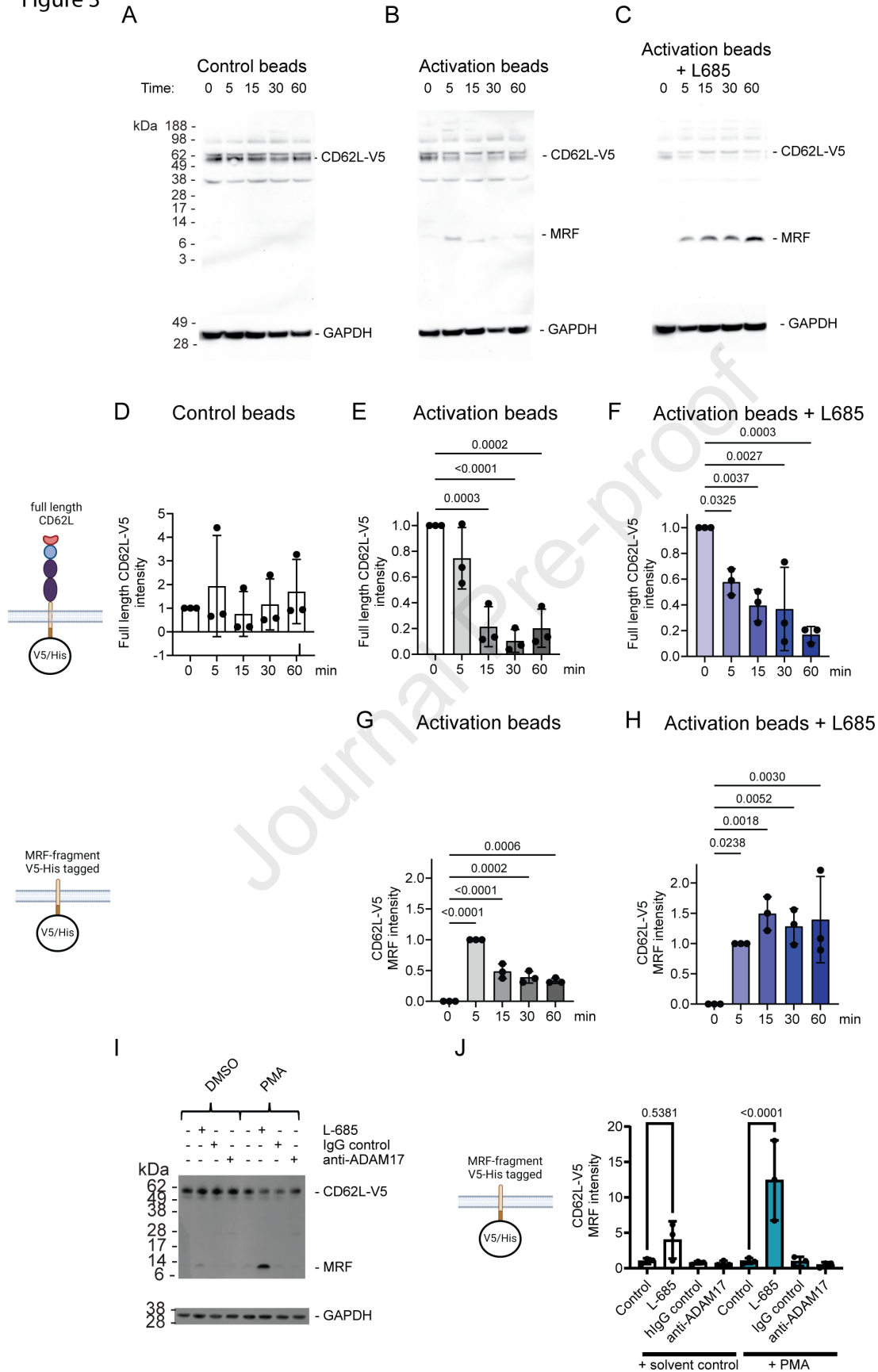


Figure 5

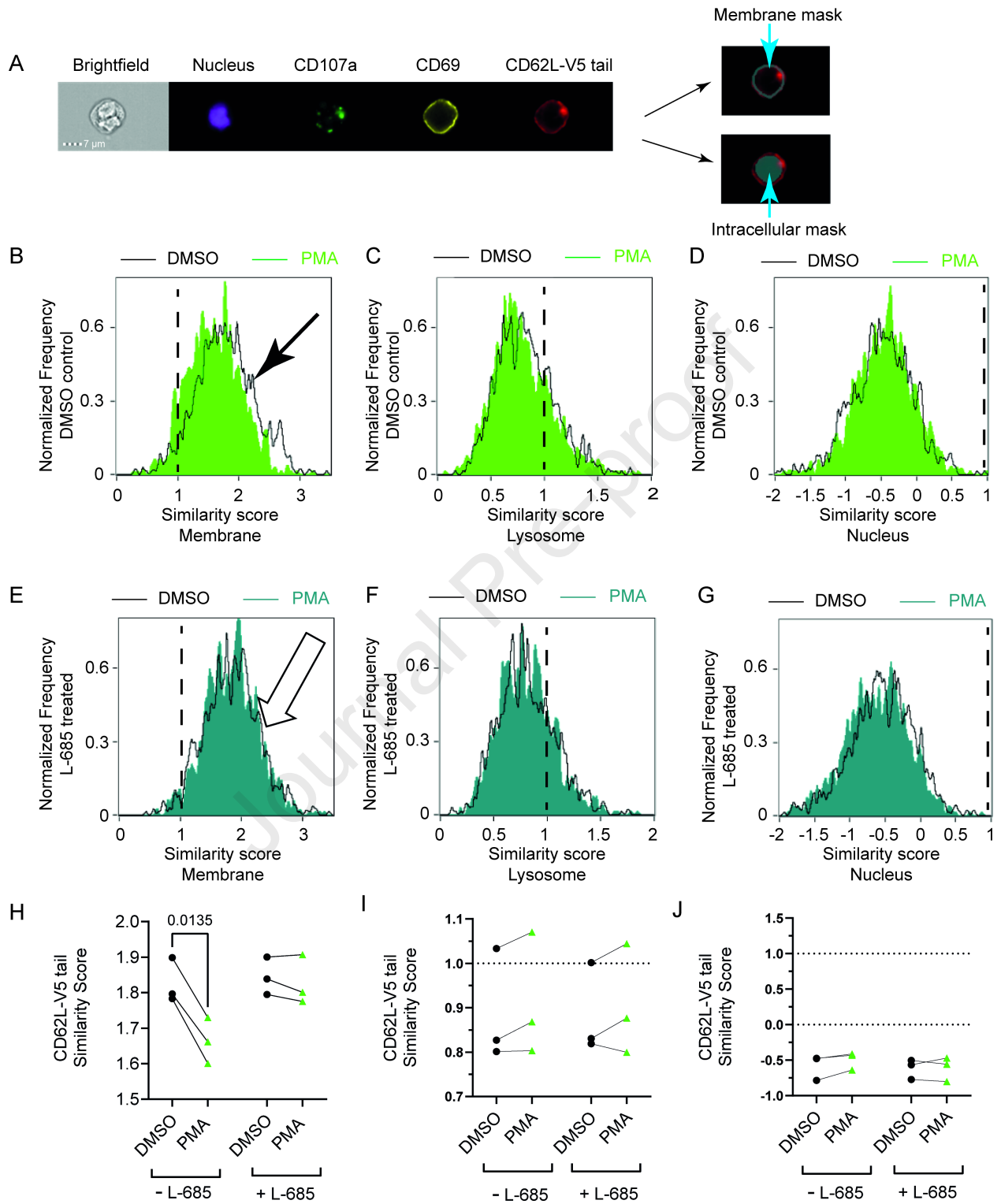


Figure 6

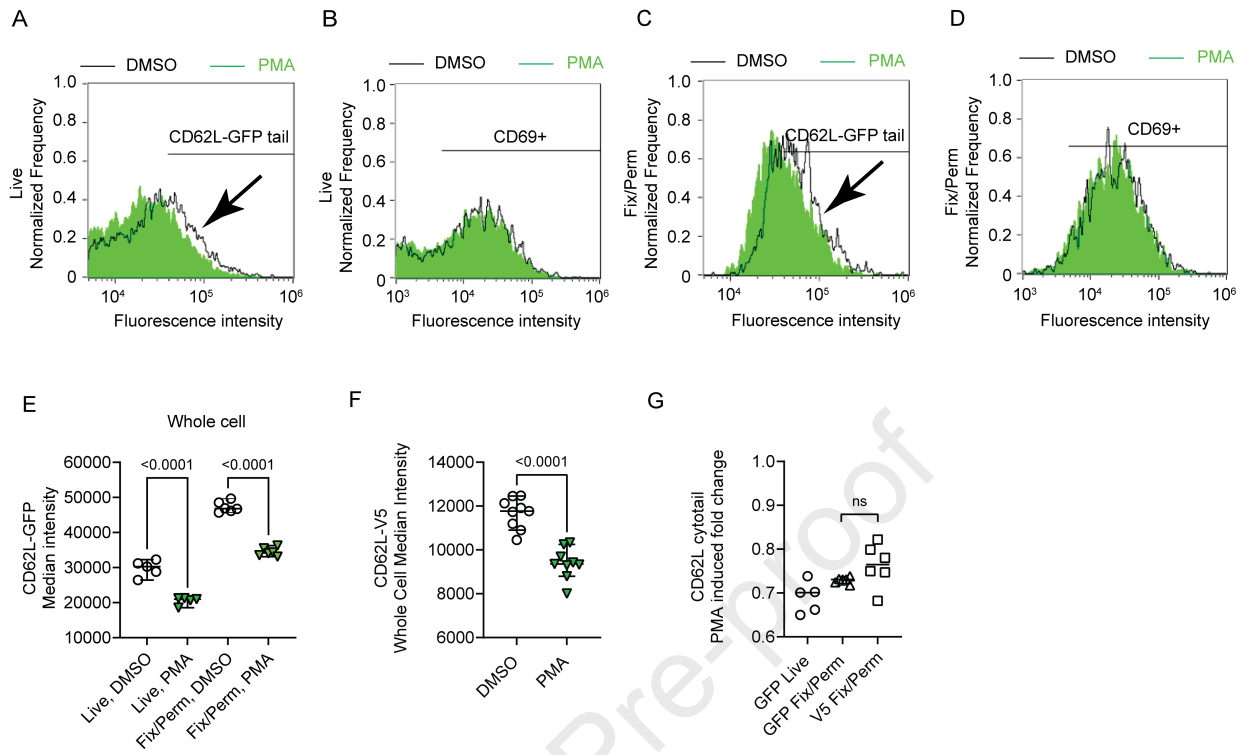
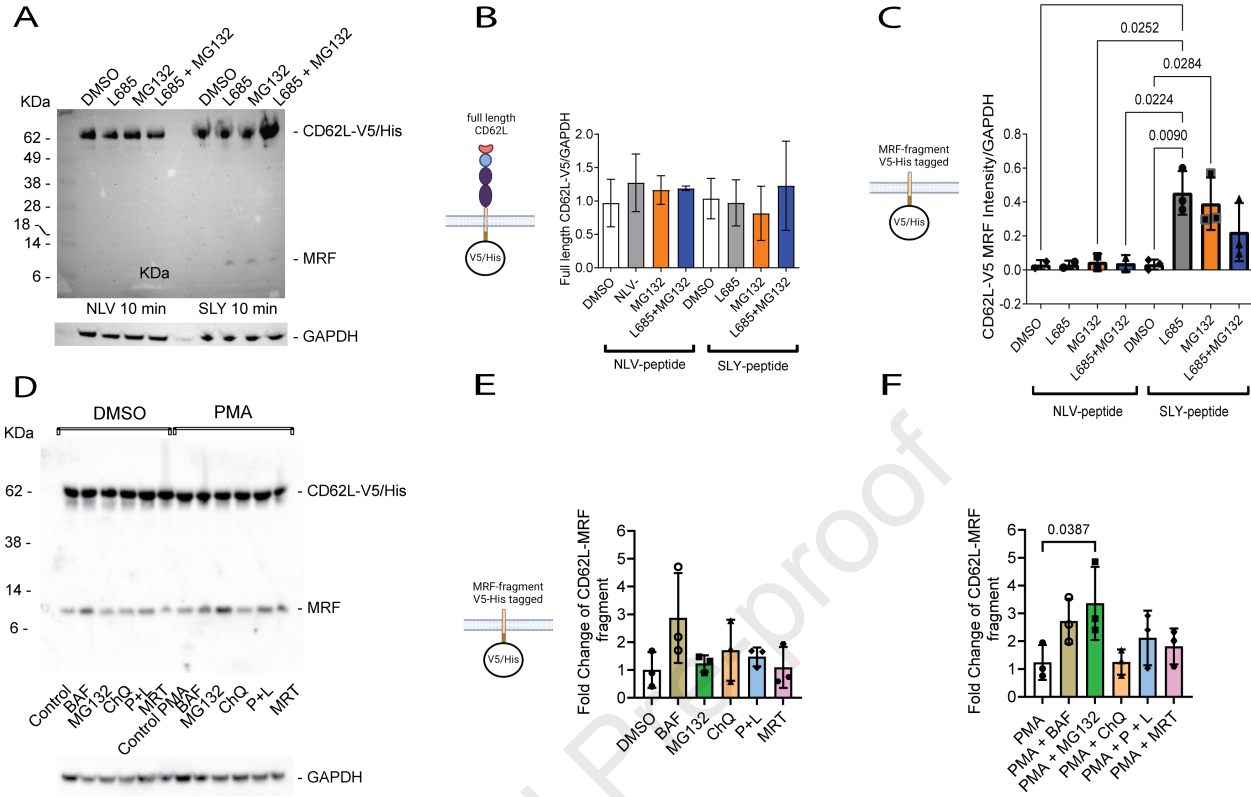
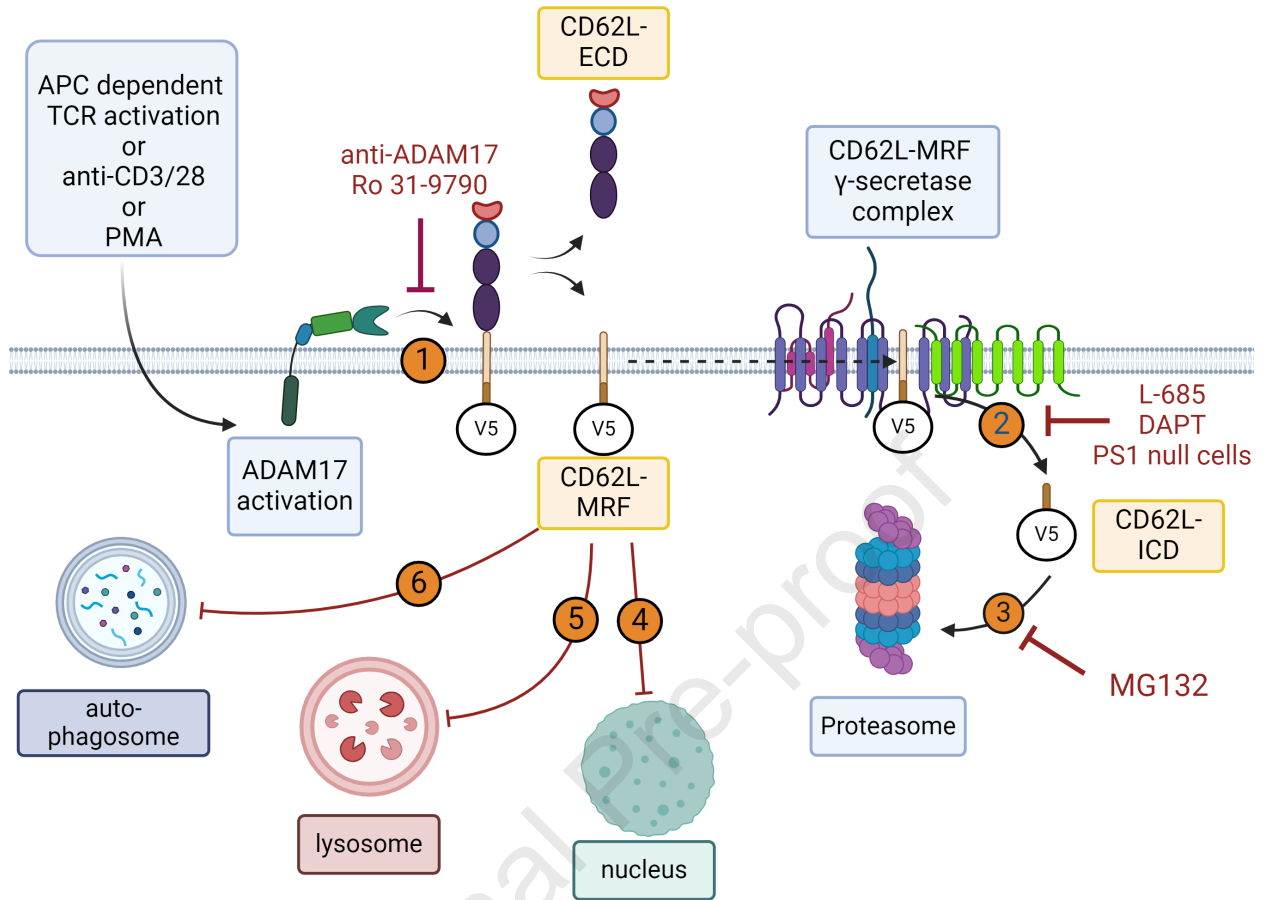


Figure 7





VK and AA conceived the study. ORM, ACN, ASA, SCW, and KB-G designed experiments, acquired and analysed data. VK and AA supervised the study with critical input from AI and DAP. ORM, ACN, VK, and AA wrote the manuscript with contributions from all authors.

Journal Pre-proof

Declaration of Interest Statement

The authors declare that they have no known competing financial interests or personal relationships that could have appeared to influence the work reported in this paper.

The author is an Editorial Board Member/Editor-in-Chief/Associate Editor/Guest Editor for this journal and was not involved in the editorial review or the decision to publish this article.

The authors declare the following financial interests/personal relationships which may be considered as potential competing interests: